

Selective Inference in Graphical Models via Maximum Likelihood

Sofia Guglielmini*

Orstat and Leuven Statistics Research Center, KU Leuven, Leuven, Belgium,
Gerda Claeskens

Orstat and Leuven Statistics Research Center, KU Leuven, Leuven, Belgium
and

Snigdha Panigrahi

Department of Statistics, University of Michigan

Abstract

The graphical lasso is a widely used algorithm for fitting undirected Gaussian graphical models. However, for inference on functionals of edge values in the learned graph, standard tools lack formal statistical guarantees, such as control of the type I error rate. In this paper, we introduce a selective inference method for asymptotically valid inference after graphical lasso selection with added randomization. We obtain a selective likelihood, conditional on the event of selection, through a change of variable on the known density of the randomization variables. Our method enables interval estimation and hypothesis testing for a wide range of functionals of edge values in the learned graph using the conditional maximum likelihood estimate. Our numerical studies show that introducing a small amount of randomization: (i) greatly increases power and yields substantially shorter intervals compared to other conditional inference methods, including data splitting; (ii) ensures intervals of bounded length in high-dimensional settings where data splitting is infeasible due to insufficient samples for inference; (iii) enables inference for a wide range of inferential targets in the learned graph, including measures of node influence and connectivity between nodes.

Keywords: Covariance estimation, Graphical models, Networks, Post-selection inference, Randomization, Selective inference

*The authors acknowledge support from project C16/20/002 of the Research Fund KU Leuven, Belgium, project ASTeRISK Research Foundation Flanders [grant number 40007517] of the Excellence of Science (EOS) program (FWO-FNRS, Belgium) and NSF CAREER Award DMS-2337882. Data are provided by OASIS (OASIS-1). Principal Investigators: D. Marcus, R. Buckner, J. Csernansky J. Morris; P50 AG05681, P01 AG03991, P01 AG026276, R01 AG021910, P20 MH071616, U24 RR021382.

1 Introduction

The graphical lasso is a popular algorithm for learning sparse, undirected Gaussian graphical models. The model assumes that the data consist of n independent and identically distributed observations $X = (X_1, \dots, X_n)^\top$, drawn from a centered p -dimensional normal distribution:

$$X_i \sim N_p(0_p, \Sigma), \quad \text{for all } i = \{1, \dots, n\}.$$

The presence or absence of edges in the graph underlying this model, where the nodes represent variables, is encoded in the precision matrix $\Theta = \Sigma^{-1}$, the inverse of the covariance. More specifically, the edge between nodes j and k is absent if and only if the (j, k) -th element of the precision matrix Θ is equal to 0; equivalently, by the pairwise Markov property, if and only if X_j and X_k are independent conditionally on the other variables in the graph.

To encourage sparsity in the number of edges of the graph, the graphical lasso imposes a penalty on the ℓ_1 -norm of the precision matrix Θ . The penalized estimator is obtained as the solution of

$$\underset{\{\Theta = \Theta^\top, \Theta \succ 0\}}{\operatorname{argmin}} \quad \{\operatorname{tr}(S_n \Theta) - \log \det(\Theta) + \lambda_n \|\Theta\|_1\}, \quad (1)$$

where $S_n = X^\top X/n$ is the sample covariance matrix and λ_n is a positive penalty parameter with asymptotic order $O(n^{-1/2})$. The optimization is carried over the class of $p \times p$ symmetric matrices that are positive definite, as denoted by $\Theta \succ 0$, and can be efficiently solved using fast iterative algorithms, such as the one proposed in Friedman et al. [2008].

In many cases, learning a graph or equivalently, estimating the zeros of the precision matrix is not the final step of the analysis. A natural inferential goal is to test the significance of the edges or to quantify uncertainty in the estimates of edge values by constructing confidence intervals. More generally, one may seek to answer questions about functionals of edge parameters in the learned graph. For example, in network analysis, practical questions involve estimating node strengths, defined as the sum of the absolute values of edge values connected to a given node, or estimating other connectivity measures between groups of

nodes in the learned graph. Such questions involve “post-selection” parameters—many examples of which are provided in the next section—that are functions of the learned graph or the entries of the estimated sparse precision matrix.

These questions cannot be addressed using naive inferential tools, which use the same data to first select parameters or their functionals and then seek answers. One simple approach to solve this problem is to use different samples for the selection and inference steps, known as data splitting [Picard and Berk, 1990]. However, this approach discards samples in both steps, leading to less accurate selection as well as reduced power in the inference step, often resulting in inadmissible tests [Fithian et al., 2017].

Modern selective inference methods overcome this challenge by preserving standard inference guarantees while allowing for the efficient use of all available data samples for both tasks. In this paper, we introduce a conditional selective inference method for edge parameters in graphs estimated using the graphical lasso. Using the likelihood-based framework in Panigrahi and Taylor [2023], Huang et al. [2023a], we develop a maximum likelihood approach for graphical models.

Our approach utilizes an external randomization scheme with additive noise to account for the selection of edge parameters. Data splitting itself is a special case of randomization, where the randomness comes in the random choice of the sample split. The external randomization in our method leads to a more powerful, data-efficient, and versatile toolbox for inference in the learned graph.

- (i) Our method yields substantially shorter confidence intervals compared to existing conditional methods, including the inefficient data-splitting approach, which often fails to provide inference in high dimensional scenarios.

Utilizing the polyhedral shape of conditioning events resulting from the lasso penalty, conditional methods by Taylor and Tibshirani [2018] and Guglielmini and Claeskens [2025] developed asymptotic inference in graphical models, with the latter extending

their method to a large class of loss and penalty functions. However, similar to the polyhedral method for the Gaussian regression problem, the confidence intervals from these methods have infinite expected length, as shown by Kivaranovic and Leeb [2021]. The additive randomization in our method always yields bounded intervals, while the previous methods may produce infinitely long intervals, as shown in our simulations.

- (ii) Our method obtains the maximum likelihood estimator (MLE) from a selective likelihood to construct inference for a wide range of functionals of edge parameters, including those used to measure connectivity and node strength in network analysis.

Our inference method is highly versatile, allowing the use of standard tools like the bootstrap or delta method to approximate quantiles of the distribution of the post-selection MLE. This facilitates interval estimation and hypothesis testing for general and potentially complex functionals of edge parameters. Note, these tasks cannot generally be achieved with a conditional approach that forms a pivot for a scalar-valued parameter. Such approaches have been developed for selective inference in different contexts, such as Lee et al. [2016], Tian and Taylor [2018], Panigrahi and Taylor [2018], Duy and Takeuchi [2021], Panigrahi et al. [2024] for lasso regression, Huang et al. [2023b] for the neighborhood lasso approach to learn graphs, Neufeld et al. [2022], Bakshi et al. [2024] for regression trees, Freidling et al. [2024] for adaptive experiments. Furthermore, tools for high-dimensional graphical lasso, such as the debiased approach in Janková and van de Geer [2015], provide intervals for all entries of the precision matrix but fail to address questions about edge values in the learned graph.

The rest of the paper is organized as follows. In Section 2, we introduce the randomized graphical lasso with additive noise and describe various post-selection inference quantities that practitioners seek to estimate in the learned graph. Section 3 presents the basic estimators in the learned graph, along with the selection event underlying the graph estimated by the graphical lasso algorithm. In Section 4, we derive the selective likelihood,

obtain the conditional MLE estimate, and explain how to compute confidence intervals and hypothesis tests using this estimate. Finally, numerical experiments in Sections 5 and 6 demonstrate our method’s performance across different types of graph data, highlighting its advantages over existing approaches in terms of coverage control, interval length, and broader applicability. The proofs of Lemma’s, Propositions and Theorems are collected in the Supplement.

2 Randomized graphical lasso

Define $d = p(p + 1)/2$ and denote by $\theta = \text{vech}(\Theta) = \text{vh}(\Theta) \in \mathbb{R}^d$ the vector-half of the symmetric matrix $\Theta \in \mathbb{R}^{p \times p}$, which collects the entries $\{\Theta_{i,j} : i \leq j\}$. Suppose that we generate a random variable $\omega_n = \omega/\sqrt{n}$, where $\omega \sim N_d(0_d, \Omega)$ with a fixed, pre-specified Ω . We then solve the randomized, regularized optimization problem

$$\hat{\Theta}_{n,\lambda_n} = \underset{\{\Theta = \Theta^T, \Theta \succ 0\}}{\text{argmin}} \{ \text{tr}((S_n - W_n)\Theta) - \log \det(\Theta) + \lambda_n \|\Theta\|_1 \}, \quad (2)$$

where W_n is such that $D_p^\top \text{vec}(W_n) = \omega_n$, and D_p is the duplication matrix such that $\text{vec}(A) = D_p \text{vh}(A)$ [Magnus and Neudecker, 1985]. In practice, W_n corresponds to the matrix version of ω_n , with the diagonal multiplied by 2. This use of the duplication matrix is also noted in Guglielmini and Claeskens [2025] and Srinivasan and Panda [2023].

Consistent with our notational scheme, let $\hat{\theta}_{n,\lambda_n} = \text{vh}(\hat{\Theta}_{n,\lambda_n})$. We denote the set of active entries of the penalized solution by

$$\hat{E} = \left\{ j \in \{1, \dots, d\} : \hat{\theta}_{n,\lambda_n} \neq 0 \right\},$$

and denote by E and E' the realized value of \hat{E} and the complement of \hat{E} , respectively.

2.1 Post-selection targets

Once a graph is learned, and a value E is observed for the set of selected edges \hat{E} , a key challenge is constructing interval estimates for various post-selection targets.

A first example of such a quantity is (a) each edge value of the learned graph, $\theta_{n,E;i}^*$, where

$$\Theta_{n,E}^* = \underset{\Theta \in \mathcal{R}_E}{\operatorname{argmin}} \mathbb{E} [\ell_n(\Theta; X)], \quad (3)$$

which is obtained after fitting the graph to the selected edges

$$\mathcal{R}_E = \{\Theta \in \mathbb{R}^{p \times p} : [\operatorname{vh}(\Theta)]_{E'} = 0_{|E'|} \text{ and } \Theta^\top = \Theta\}. \quad (4)$$

The function ℓ_n denotes the loss, see (2), i.e., negative log-likelihood.

A question that often comes up in graphical modelling is giving a measure of importance, or *centrality* to each node in the graph [Freeman, 1978]. Finding the most important nodes is useful in psychology for targeted therapy and observation of warning signs; in biological settings, the structure of the most central molecules can help predict fluctuations in phenotypes, the observed features of the cells [del Rio et al., 2009]. The *centrality* of a node in a graph depends on how connected it is to the other nodes. In a weighted graph, such as the Gaussian graphical model, a measure of centrality of a node j is its (b) *node strength* [Barrat et al., 2004], the sum of the absolute values of the edge parameter values that are connected to node j :

$$NS_E(j) = \sum_{i \in E_j} |\theta_{n,E;i}^*|,$$

where the edges in the selected set E which have one endpoint in j have index in E_j .

Robinaugh et al. [2016] introduced two measures of *expected influence* in the context of networks of interdependent symptoms in complicated grief. As is most often the case, some of the edges in the network will have positive sign and some have negative sign. In such networks, edges can have both positive and negative signs, meaning some symptoms contribute positively to overall network activation (the sum of symptom levels, representing grief intensity), while others contribute negatively. A node may have high centrality but, if its positive and negative effects balance out, it may not be *influential*. Two measures are proposed: (c) the one-step expected influence (similar to node strength, without taking

the absolute value):

$$EI_E^{(1)}(j) = \sum_{i \in E_j} \theta_{n,E;i}^*$$

and (d) the two-step expected influence:

$$EI_E^{(2)}(j) = EI_E^{(1)}(j) + \sum_{i=1, i \neq j}^p \Theta_{n,E;i,j}^* EI_E^{(1)}(i) = A_1 \theta_{n,E}^* + \theta_{n,E}^{*\top} A_2^\top B_2 \theta_{n,E}^* = f_2(\theta_{n,E}^*),$$

for appropriately defined matrices A_1 , A_2 and B_2 . Node strength and expected influence are examples of what Sporns [2011], among others, calls measures of influence, identifying them as one of the main aspects of a brain network analysis.

In many networks, it is possible to identify a *community structure*, with communities (or *modules*) of nodes with common feature or function and a higher density of connections within them, rather than between them. For example, brain networks present densely connected modules, based on both anatomical and functional characteristics [Sporns, 2011]. In any type of network, different modules are typically interacting parts of a larger network and *bridging* nodes [Castro et al., 2019] help analyze the dependence relationships of nodes in different modules. The (e) bridge strength of node i in a community c is the sum of the absolute weights of nodes that connect node i to nodes in any other community, therefore defined as

$$BS_E(j) = \sum_{i \in E_j^{(b)}} |\theta_{n,E;i}^*|,$$

where the edges in the selected set E which have one endpoint in j and the other in a community which j does not belong to have index in $E_j^{(b)}$.

Analogously, (f) the bridge expected influence is analogous to bridge strength, with the difference that the edge values are summed without first taking the absolute values [Jones et al., 2021]:

$$BI_E(j) = \sum_{i \in E_j^{(b)}} \theta_{n,E;i}^*$$

Finally, another question of interest is the difference between two nodes in terms of these metrics. We can, for example, consider (g) the difference in strength between nodes j and

k :

$$SD_E(j, k) = \sum_{i \in E_j} |\theta_{n,E;i}^*| - \sum_{i \in E_k} |\theta_{n,E;i}^*|.$$

Next, we describe our framework and method that provides interval estimates for all the post-selection targets listed here and, more broadly, for a continuous functional of edge values in the learned graph.

3 Our framework

3.1 Refitted estimators

After selecting with the randomized graphical lasso in (1), we obtain the maximum likelihood estimator in the selected model, which we call the refitted MLE. This estimator is obtained by refitting the model with the constraints that the elements with indices in E' are set to 0, i.e., we solve

$$\bar{\Theta}_{n,E} = \operatorname{argmin}_{\Theta \in \mathcal{R}_E} \{\ell_n(\Theta; X)\},$$

where \mathcal{R}_E as defined in (4) and the minimizer $\bar{\Theta}_{n,E}$ is the refitted MLE. Let $\bar{\theta}_n = \operatorname{vh}(\bar{\Theta}_{n,E})$ be the vector-half representation of the refitted MLE.

We define the $d \times d$ matrices

$$H(\Theta_{n,E}^*) = \mathbb{E} \left[n^{-1} \frac{\partial^2 \ell_n(\Theta_{n,E}^*; X)}{\partial \operatorname{vh}(\Theta) \partial \operatorname{vh}(\Theta)^\top} \right] \text{ and } J(\Theta_{n,E}^*) = \mathbb{E} \left[n^{-1} \frac{\partial \ell_n(\Theta_{n,E}^*; X)}{\partial \operatorname{vh}(\Theta)} \frac{\partial \ell_n(\Theta_{n,E}^*; X)}{\partial \operatorname{vh}(\Theta)}^\top \right],$$

where

$$\frac{\partial \ell_n(\Theta_{n,E}^*; X)}{\partial \operatorname{vh}(\Theta)} = \frac{\partial \ell_n(\Theta; X)}{\partial \operatorname{vh}(\Theta)} \Big|_{\Theta = \Theta_{n,E}^*}, \quad \frac{\partial^2 \ell_n(\Theta_{n,E}^*; X)}{\partial \operatorname{vh}(\Theta) \partial \operatorname{vh}(\Theta)^\top} = \frac{\partial^2 \ell_n(\Theta; X)}{\partial \operatorname{vh}(\Theta) \partial \operatorname{vh}(\Theta)^\top} \Big|_{\Theta = \Theta_{n,E}^*}.$$

Analogously, we define their sample versions

$$H_n(\Theta_{n,E}^*) = n^{-1} \sum_{h=1}^n \frac{\partial^2 \ell_n(\Theta_{n,E}^*; X_h)}{\partial \operatorname{vh}(\Theta) \partial \operatorname{vh}(\Theta)^\top} \text{ and } J_n(\Theta_{n,E}^*) = n^{-1} \sum_{h=1}^n \left[\frac{\partial \ell_n(\Theta_{n,E}^*; X_h)}{\partial \operatorname{vh}(\Theta)} \frac{\partial \ell_n(\Theta_{n,E}^*; X_h)}{\partial \operatorname{vh}(\Theta)}^\top \right]$$

Then, we obtain the following result.

Lemma 1. $J_n(\Theta_n) - J(\Theta_n^*) = o_P(1)$ and $H_n(\Theta_n) - H(\Theta_n^*) = o_P(1)$, as $n \rightarrow \infty$ and where Θ_n is a consistent estimator of Θ_n^* , by the law of large numbers.

Without loss of generality, we regroup the entries of any $d \times d$ matrix M , such that the row and column indices for a given set E appear in the top left submatrix. We define the following partitioning $M = \begin{pmatrix} M_{EE} & M_{EE'} \\ M_{EE'} & M_{E'E'} \end{pmatrix} = \begin{pmatrix} M_E & M_{E'} \end{pmatrix}$. Analogously, for any $d \times 1$ vector θ , θ_E is the set of elements of θ indexed by E .

Lemma 2. The matrix $H_{n,EE}(\widehat{\Theta}_{n,E})$, where $\widehat{\Theta}_{n,E}$ is any positive definite estimator of $\Theta_{n,E}^*$, is positive definite. Furthermore, if $n \geq |E|$, the matrix $J_{n,EE}(\widehat{\Theta}_{n,E})$ is also positive definite.

If $n < |E|$, $J_{n,EE}(\widehat{\Theta}_{n,E})$ is singular. In this case, $J_n(\widehat{\Theta}_{n,E})$ can in practice be substituted by the invertible $H_n(\widehat{\Theta}_{n,E})$. If the data come from a Gaussian distribution, these matrices are asymptotically equivalent by the second Bartlett identity.

We now obtain the asymptotic distribution of the refitted MLE, fixing the selected graph or equivalently, fixing the set E .

Proposition 1. Define the nonsingular, positive definite matrices

$\Sigma_{n,E} = H_{n,EE}^{-1}(\Theta_{n,E}^*) J_{n,EE}(\Theta_{n,E}^*) H_{n,EE}^{-1}(\Theta_{n,E}^*)$ and $\Sigma_E = \lim_{n \rightarrow \infty} \Sigma_{n,E}$. Then, for a fixed set E ,

$$n^{1/2}(\bar{\theta}_{n,E} - \theta_{n,E}^*) \xrightarrow{d} N_{|E|}(0_{|E|}, \Sigma_E).$$

For ease of notation, we do not further denote the dependence of the matrices $H_n(\Theta_{n,E}^*)$ and $J_n(\Theta_{n,E}^*)$ and their submatrices on $\Theta_{n,E}^*$.

The selection procedure, however, does not depend on $\bar{\theta}_n$ alone. In Lemma 3, we identify an additional refitted estimator such that the selection procedure relies on the data through both of these refitted estimators.

Lemma 3. Under the assumption of Proposition 1, and with $A_E = H_{n,E'E} - J_{n,E'E} J_{n,EE}^{-1} H_{n,EE}$, define the vectors $\bar{\theta}_{n,E'}^\perp = n^{-1} \frac{\partial \ell_n(\bar{\Theta}_{n,E}; X)}{\partial \text{vh}(\Theta)_{E'}} - A_E \bar{\theta}_{n,E}$ and $\theta_{n,E}^{1*} = n^{-1} \mathbb{E} \left[\frac{\partial \ell_n(\Theta_{n,E}^*; X)}{\partial \text{vh}(\Theta)_{E'}} \right] -$

$A_E \theta_{n,E}^*$. Then, with $\Sigma_E^\perp = J_{n,E'E'} - J_{n,E'E} J_{n,EE}^{-1} J_{n,EE'}$,

$$\sqrt{n}(\bar{\theta}_{n,E}^\perp - \theta_{n,E}^{\perp*}) \xrightarrow{d} N_{|E'|}(0_{|E'|}, \Sigma_{E^\perp}).$$

Furthermore, $\bar{\theta}_{n,E'}^\perp$ and $\bar{\theta}_{n,E}^\perp$ are orthogonal and thus independent under the asymptotic normal distribution.

3.2 The selection event

We now characterize the selection event $\{\widehat{E} = E\}$ in terms of the randomized graphical lasso estimators obtained by solving (2).

In order to obtain a tractable conditional distribution, we take a proper subset of this event,

$$\left\{ \widehat{E} = E, \widehat{S} = S, \widehat{U} = U \right\} = \left\{ \widehat{S} = S, \widehat{U} = U, \sqrt{n}B \in \mathbb{R}_+^{|E|} \right\}, \quad (5)$$

where

$$\begin{aligned} B &\in \mathbb{R}^{|E|}; & b_j &= |\widehat{\theta}_{n,\lambda_n}(j)| & \text{for } j \in E; \\ S &\in \mathbb{R}^{|E|}; & s_j &= \text{sign}(\widehat{\theta}_{n,\lambda_n}(j)) & \text{for } j \in E; \\ U &\in \mathbb{R}^{|E'|}; & u_{j'} &\in [-1, 1] & \text{for } j' \in E', \end{aligned}$$

and $\widehat{\theta}_{n,\lambda_n}(j)$ denotes the j^{th} component of the randomized graphical lasso estimator.

The event on the left-hand side is equivalent to conditioning on the subgradient of the lasso penalty, as was done for the least squares regression problem in Panigrahi et al. [2024]. Further conditioning on a proper subset of the selection event, which is equivalent to conditioning on additional information about the randomized graphical lasso estimators, always guarantees valid selective inference. Even with this additional conditioning, it is important to note that, unlike data splitting, we do not condition on the entire dataset used for selection. Consequently, as our simulations demonstrate, our interval estimates are generally much shorter than those obtained through the inefficient data splitting approach.

4 Randomized selective inference

In this section, we outline the steps for constructing confidence intervals and tests using an asymptotic post-selection likelihood. We first present this likelihood, followed by our approach to conducting inference based on it.

4.1 Randomization map

Starting from the optimization problem in (2), using the Karush-Kuhn-Tucker conditions and first-order Taylor expansions, in Proposition 2, we define a map $\Pi_{\theta, \theta^\perp}$ that relates the randomized graphical lasso estimators (B, U) to ω_n . This relationship is key to deriving the likelihood using the selected model. To simplify our notation, we define

$$\bar{\theta}_\perp = (0_{|E|}^\top, \bar{\theta}_{n,E}^{\perp\top})^\top \quad \text{and} \quad \theta_\perp^* = (0_{|E|}^\top, \theta_{n,E}^{\perp*\top})^\top.$$

Proposition 2. *Define the map $\Pi_{\theta, \theta^\perp} : \mathbb{R}^{|E|} \times \mathbb{R}^d \rightarrow \mathbb{R}^d : (b, u) \mapsto C_1\theta + C_2b + f(u, \theta^\perp)$,*

where $C_1 = -J_{n,E}J_{n,EE}^{-1}H_{n,EE}$, $C_2 = H_{n,E}\text{diag}(S)$, $f(U; \sqrt{n}\theta_\perp) = \frac{\sqrt{n}}{2}D_p^\top \text{vec}(\hat{\mathcal{P}}') + \sqrt{n}\theta_\perp$

and $\hat{\mathcal{P}}'$ is such that $\text{vh}(\hat{\mathcal{P}}')_j = \begin{cases} \lambda_n S_j & \text{if } j \in E, \\ \lambda_n U_j & \text{if } j \in E'. \end{cases}$ Then,

$$\sqrt{n}\omega_n = \Pi_{\sqrt{n}\bar{\theta}_{n,E}, \sqrt{n}\bar{\theta}_\perp}(\sqrt{n}B, U) + o_P(1).$$

From here on, we denote the closely related vector $\sqrt{n}\bar{\omega}_n = \Pi_{\sqrt{n}\bar{\theta}_{n,E}, \sqrt{n}\bar{\theta}_\perp}(\sqrt{n}B, U)$.

For randomized group lasso selection in the regression model, a similar representation was obtained by Huang et al. [2023a], see also Panigrahi et al. [2023]. The argumentation is here for Gaussian graphical models with emphasis on the precision matrix, not for a regression model as in Huang et al. [2023a]. Consequently, the selection event and the parameterizations are also different.

4.2 Selective likelihood

We form a likelihood based on the conditional distribution of the refitted MLE

$$\sqrt{n}\bar{\theta}_{n,E} \left| \left\{ \widehat{S} = S, \widehat{U} = U, \sqrt{n}B \in \mathbb{R}_+^{|E|}, \bar{\theta}_{n,E}^\perp = \theta_{n,E}^\perp \right\}, \quad (6)$$

where $\left\{ \widehat{S} = S, \widehat{U} = U, \sqrt{n}B \in \mathbb{R}_+^{|E|} \right\}$ is the selection event in (5). By further conditioning on $\bar{\theta}_{n,E}^\perp$ in this distribution, we eliminate the nuisance parameters $\theta_{n,E}^{\perp*}$ from the post-selection likelihood, rendering it a function of $\theta_{n,E}^*$ alone.

In order to derive the conditional distribution in (6), we consider the distribution of

$$\sqrt{n}(\bar{\theta}_{n,E}^\top, B^\top)^\top \left| \left\{ \widehat{S} = S, \widehat{U} = U, \bar{\theta}_{n,E}^\perp = \theta_{n,E}^\perp \right\},$$

with pre-selection likelihood $L_{n,S,U,\theta_{n,E}^\perp}(\theta_{n,E}^*, \theta_\perp^*; \bar{\theta}_{n,E}, B)$, truncated to the event $\{B \in \mathbb{R}_+^{|E|}\}$.

The conditional likelihood of interest is then

$$\frac{L_{n,S,U,\theta_{n,E}^\perp}(\theta_{n,E}^*, \theta_\perp^*; \bar{\theta}_{n,E}, B) \mathbb{1}_{\mathbb{R}_+^{|E|}}(\sqrt{n}B)}{\int L_{n,S,U,\theta_{n,E}^\perp}(\theta_{n,E}^*, \theta_\perp^*; \tilde{\theta}, \tilde{B}) \mathbb{1}_{\mathbb{R}_+^{|E|}}(\sqrt{n}\tilde{B}) d\tilde{\theta} d\tilde{B}} = \frac{L_{n,S,U,\theta_{n,E}^\perp}(\theta_{n,E}^*, \theta_\perp^*; \bar{\theta}_{n,E}, B) \mathbb{1}_{\mathbb{R}_+^{|E|}}(\sqrt{n}B)}{\mathbb{P}[\sqrt{n}B \in \mathbb{R}_+^{|E|} \mid \bar{\theta}_\perp = \theta_\perp, \widehat{S} = S, \widehat{U} = U]},$$

with the log-likelihood

$$\log L_{n,S,U,\theta_{n,E}^\perp}(\theta_{n,E}^*, \theta_\perp^*; \bar{\theta}_{n,E}, B) - \log \mathbb{P}[\sqrt{n}B \in \mathbb{R}_+^{|E|} \mid \bar{\theta}_\perp = \theta_\perp, \widehat{S} = S, \widehat{U} = U].$$

We first derive the asymptotic pre-selection density for fixed selection set E and signs S ; then we obtain the conditional density by truncating the pre-selection density to the selection event; and finally, we show how we perform the numerical computation of the relevant quantities from this conditional likelihood.

Pre-selection likelihood. Consider the following assumption.

Assumption 1. *There is a sample size n_0 such that for all $n \geq n_0$ the distribution of*

$$\sqrt{n}((\bar{\theta}_{n,E} - \theta_{n,E}^*)^\top, (\bar{\theta}_{n,E}^\perp - \theta_{n,E}^{\perp*})^\top, \bar{\omega}_n^\top)^\top$$

admits a Lebesgue density g_n .

Proposition 3. *Under Assumption 1, the density of*

$$(\sqrt{n}\bar{\theta}_{n,E}^\top, \sqrt{n}(\bar{\theta}_{n,E}^\perp)^\top, \sqrt{n}B^\top, U^\top)^\top$$

is, up to a multiplicative constant, proportional to

$$g_n(\sqrt{n}(\bar{\theta}_{n,E} - \theta_{n,E}^*), \sqrt{n}(\bar{\theta}_{n,E}^\perp - \theta_{n,E}^{\perp*}), \Pi_{\sqrt{n}\bar{\theta}_{n,E}, \sqrt{n}\bar{\theta}_\perp}(\sqrt{n}B, U)),$$

From asymptotic normality and independence, for a fixed set E ,

$$\sqrt{n} \begin{pmatrix} \bar{\theta}_{n,E} - \theta_{n,E}^* \\ \bar{\theta}_{n,E}^\perp - \theta_{n,E}^{\perp*} \\ \bar{\omega}_n \end{pmatrix} \xrightarrow{d} N_{2d} \left(\begin{pmatrix} 0_{|E|} \\ 0_{|E'|} \\ 0_d \end{pmatrix}, \begin{pmatrix} \Sigma_E & 0_{|E|,|E'|} & 0_{|E|,d} \\ 0_{|E'|,|E|} & \Sigma_E^\perp & 0_{|E'|,d} \\ 0_{d,|E|} & 0_{d,|E'|} & \Omega \end{pmatrix} \right).$$

This suggests that that we can replace the pre-selection density g_n in Proposition 3 with the normal density function based on the limiting pre-selection normal distribution for $\sqrt{n}((\bar{\theta}_{n,E} - \theta_{n,E}^*)^\top, (\bar{\theta}_{n,E}^\perp - \theta_{n,E}^{\perp*})^\top, \bar{\omega}_n^\top)^\top$.

Truncated likelihood. Truncating the pre-selection density to the selection event yields our selective likelihood, which is derived next.

Theorem 1. *Using the asymptotic density and further conditioning on the nuisance vector, the law of*

$$\sqrt{n}(\bar{\theta}_{n,E}^\top, B^\top)^\top \{ \widehat{S} = S, \widehat{U} = U, \bar{\theta}_\perp = \theta_\perp \}, \quad (7)$$

truncated to the event $\{B \in \mathbb{R}_+^{|E|}\}$ is proportional to

$$\frac{\rho(\sqrt{n}\bar{\theta}_{n,E}; L\sqrt{n}\theta_{n,E}^* + m, Z)\rho(\sqrt{n}B; P\sqrt{n}\bar{\theta}_{n,E} + q, \Delta)\mathbb{1}_{\mathbb{R}_+^{|E|}}(\sqrt{n}B)}{\int \rho(\sqrt{n}\tilde{\theta}; L\sqrt{n}\theta_{n,E}^* + m, Z)\rho(\sqrt{n}\tilde{B}; P\sqrt{n}\tilde{\theta} + q, \Delta)\mathbb{1}_{\mathbb{R}_+^{|E|}}(\sqrt{n}\tilde{B})d\tilde{\theta}d\tilde{B}} \quad (8)$$

where $\rho(x; \mu, \Sigma)$ is the density of a multivariate normal variable with mean μ and covariance matrix Σ , evaluated at x , and

$$\Delta = (C_2^\top \Omega^{-1} C_2)^{-1} \quad P = -\Delta C_2^\top \Omega^{-1} C_1; \quad q = -\Delta C_2^\top \Omega^{-1} f(U; \sqrt{n}\bar{\theta}_\perp);$$

$$Z = (\Sigma_E^{-1} - P^\top \Delta^{-1} P + C_1^\top \Omega^{-1} C_1)^{-1}; \quad L = Z \Sigma_E^{-1}; \quad m = Z(P^\top \Delta^{-1} q - C_1^\top \Omega^{-1} f(U; \sqrt{n}\bar{\theta}_\perp)).$$

Numerical computation. In Theorem 1, we derive an expression for the selective likelihood, using the distribution of the randomized graphical lasso estimators and the refitted estimators in the selected model. However, in practice, computing this likelihood requires calculating the normalizing constant, which is not available in closed form. We turn to a numerical strategy to efficiently compute this normalizing constant.

We approximate the integral

$$\int \rho(\sqrt{n}\tilde{\theta}; L\sqrt{n}\theta_{n,E}^* + m, Z)\rho(\sqrt{n}\tilde{B}; P\sqrt{n}\tilde{\theta} + q, \Delta)\mathbb{1}_{\mathbb{R}_+^{|E|}}(\sqrt{n}\tilde{B})d\tilde{\theta}d\tilde{B}$$

in the normalizing constant of our selective likelihood by its Laplace approximation

$$\inf_{\theta, b \in \mathbb{R}_+^{|E|}} \left\{ \frac{1}{2}(\sqrt{n}\theta - L\sqrt{n}\theta_{n,E}^* - m)^\top Z^{-1}(\sqrt{n}\theta - L\sqrt{n}\theta_{n,E}^* - m) + \frac{1}{2}(\sqrt{nb} - P\sqrt{n}\theta - q)^\top \Delta^{-1}(\sqrt{nb} - P\sqrt{n}\theta - q) \right\}.$$

Instead of the optimization above, we solve an unconstrained version of the same problem by introducing a barrier function $\phi(\nu) = -\sum_{h=1}^{|\nu|} \log(\nu_h - c)$, in the optimization objective, which enforces the linear constraints $\nu_h > c$. To sum up, for $\mathcal{K} = [c, \infty)^{|E|}$, where we take $c = 0$ or close to 0, we replace the normalizing constant by

$$\inf_{\theta, b} \left\{ \frac{1}{2}(\sqrt{n}\theta - L\sqrt{n}\theta_{n,E}^* - m)^\top Z^{-1}(\sqrt{n}\theta - L\sqrt{n}\theta_{n,E}^* - m) + \frac{1}{2}(\sqrt{nb} - P\sqrt{n}\theta - q)^\top \Delta^{-1}(\sqrt{nb} - P\sqrt{n}\theta - q) + \phi_{\mathcal{K}}(\sqrt{nb}) \right\}.$$

The theoretical justification for this approximation, as derived in Huang et al. [2023a], comes from a large deviations-type approximation, which we include in the Supplement for completeness.

This gives us the computed log-likelihood function, which equals

$$\log \rho(\sqrt{n}\bar{\theta}_{n,E}; L\sqrt{n}\theta_{n,E}^* + m, Z) + \inf_{\theta, b} \left\{ \frac{1}{2}(\sqrt{n}\theta - L\sqrt{n}\theta_{n,E}^* - m)^\top Z^{-1}(\sqrt{n}\theta - L\sqrt{n}\theta_{n,E}^* - m) + \frac{1}{2}(\sqrt{nb} - P\sqrt{n}\theta - q)^\top \Delta^{-1}(\sqrt{nb} - P\sqrt{n}\theta - q) + \phi_{\mathcal{K}}(\sqrt{nb}) \right\}. \quad (9)$$

4.3 Confidence intervals and tests

Theorem 2. *Using the definitions as in Theorem 1, the selective MLE is*

$$\sqrt{n}\tilde{\theta}_{n,E} = L^{-1}\sqrt{n}\bar{\theta}_{n,E} + L^{-1}ZP^\top\Delta^{-1}(P\sqrt{n}\bar{\theta}_{n,E} + q - \sqrt{n}\widehat{B}) - L^{-1}m,$$

where $\widehat{B} = \operatorname{argmin}_{\widehat{B}} \left\{ \frac{1}{2}(\sqrt{n}\widehat{B} - P\sqrt{n}\bar{\theta}_{n,E} - q)^\top \Delta^{-1}(\sqrt{n}\widehat{B} - P\sqrt{n}\bar{\theta}_{n,E} - q) + \phi_{\mathcal{K}}(\sqrt{n}\widehat{B}) \right\}$, and the observed Fisher information is

$$[\tilde{I}_{n,E}]^{-1} = L^{-1}ZL^\top{}^{-1} + L^{-1}Z[P^\top\Delta^{-1}P - P^\top\Delta^{-1}(\Delta^{-1} + \nabla^2\phi_{\mathcal{K}}(\widehat{B}))^{-1}\Delta^{-1}P]ZL^\top{}^{-1}.$$

Algorithm 1 details the necessary steps to obtain these quantities, starting from the observed data.

Inference using approximate asymptotic distribution. We can then take a normal approximation using the results in Theorem 2 for the mean and the variance:

$$\sqrt{n}(\tilde{\theta}_{n,E} - \theta_{n,E}^*) \sim N_{|E|}(0_{|E|}, [\tilde{I}_{n,E}]^{-1}). \quad (10)$$

Case (a). Confidence intervals and significance tests for the selected edges can be constructed using the result in (10) directly.

Case (c). The one-step expected influence is estimated as $\widehat{EI}_E^{(1)}(j) = \sum_{i \in E_j} \tilde{\theta}_{n,E;i}$, a linear combination of the post-selection edge values. Then, its selective distribution is

$$\sqrt{n} \left(\widehat{EI}_E^{(1)}(j) - EI_E^{(1)}(j) \right) \sim N \left(0, \sum_{i,j \in E_j} [\tilde{I}_{n,E}]_{ij}^{-1} \right). \quad (11)$$

Case (d). The estimate for the two-step expected influence is $\widehat{EI}_E^{(2)}(j) = f_2(\tilde{\theta}_{n,E})$. Then, using the multivariate delta method, the selective distribution is

$$\sqrt{n} \left(\widehat{EI}_E^{(2)}(j) - EI_E^{(2)}(j) \right) \sim N \left(0, f_2'(\tilde{\theta}_{n,E})^\top \tilde{I}_{n,E}^{-1} f_2'(\tilde{\theta}_{n,E}) \right),$$

where $f_2'(\theta) = A_1 + (A_2^\top B_2 + B_2^\top A_2)\theta$.

Case (f). For a given set of communities, where node j belong to community c_1 , the distribution of the bridge expected influence of node j is defined as in (11), substituting $E_j^{(b)}$ for E_j .

Algorithm 1 Obtain the selective maximum likelihood estimate and Fisher information matrix. The computation of the necessary quantities is detailed in Table 5 in the Supplement.

Require: Scaled, centered data matrix X of size $n \times p$

Require: Fixed penalty $\lambda_n = O_p(n^{-1/2})$

Require: Randomization variance matrix Ω of size $d \times d$, where $d = p(p+1)/2$

Ensure: Selective maximum likelihood estimate $\tilde{\theta}_E$ and Fisher information matrix \tilde{I}^{-1}

Generate $\omega \sim N_d(0_d, \Omega)$

$W_n \leftarrow \text{vh}^{-1}(\omega/\sqrt{n})$

$\text{diag}(W_n) \leftarrow 2\text{diag}(W_n)$.

$S_n \leftarrow X^\top X/n$

$\hat{\Theta} \leftarrow \text{GRAPHICALASSO}(S_n - W_n, \lambda_n)$

$\bar{\Theta} \leftarrow \text{CONSTRAINEDMLE}(S_n, \bar{\Theta}_{E'} = 0)$

for each j from 1 to d **do**

subgrad $_j \leftarrow -\ell'_j + \omega_{n,j}$ ▷ Penalty (sub)gradient using the KKT conditions

end for

Compute the quantities in Table 5

$\hat{b} \leftarrow \text{argmin}_b \{b^\top \Delta^{-1} b/2 - b^\top \Delta^{-1} (P(\sqrt{n}\bar{\theta}_E) + \sqrt{n}q) - \sum_{j=1}^{|E|} \log(b_j)\}$

$\tilde{\theta}_E \leftarrow L^{-1}\bar{\theta}_E + L^{-1}ZP^\top \Delta^{-1} (P\bar{\theta}_E + q - \hat{b}/\sqrt{n}) - L^{-1}m$

$\tilde{I}^{-1} \leftarrow L^{-1}ZL^{-1\top} + L^{-1}Z[P^\top \Delta^{-1} P - P^\top \Delta^{-1} (\Delta^{-1} + \text{diag}(1/\hat{b}^2))^{-1} \Delta^{-1} P]Z(L^{-1\top})$

Inference using the constrained parametric bootstrap test. If the functional is not differentiable, rendering the delta method inapplicable, we demonstrate how the constrained bootstrap can be used to approximate the distribution of the MLE.

Case (b). We now consider the measures of node strength, which take the form of the \sqrt{n} -bounded estimator $\hat{t}(\tilde{\theta}_{n,E}) = \sum_{i \in E_j} |\tilde{\theta}_{n,E;i}|$ (see Lemma 4 in the online Appendix). These metrics are functions on the absolute value of the estimated edge parameters.

Suppose we have a null hypothesis $H_0 : t(\theta_{n,E}^*) = t_0$. Define then the test statistic $g_0(X)$, which depends on the data and on the null value, and has distribution F_0 under the null hypothesis. In particular, we define $g_0(X) = G_0(t(\tilde{\theta}_{n,E}))$, where

$$G_0(t) = \int_{A_0} \rho(\sqrt{n}\theta, \sqrt{n}\theta_0, [\tilde{I}_{n,E}]^{-1}) d\theta, \quad (12)$$

where $A_0 = \{\theta : \sum_{i \in E_j} |\theta_i| \leq t\} = \{\theta : t(\theta) \leq t\}$, $\theta_0 \in \{\theta : \sum_{i \in E_j} |\theta_i| = t_0\} = \{\theta : t(\theta) = t_0\}$. In other words, $G_0(t) = P_0(t(\tilde{\theta}_{n,E}) \leq t)$, therefore G_0 is the cumulative distribution function of $t(\tilde{\theta}_{n,E})$ under the null hypothesis H_0 , which is incorporated by ensuring that the mean of the normal density is such that the null hypothesis holds true. Therefore, this is a pivotal quantity, with null distribution $U(0, 1)$.

In practice, it is very difficult to obtain a numerical result for the integral in (12) in realistic time. We thus consider a Monte Carlo approach, which results in a parametric bootstrap p-value. Null-resampling, whenever possible, is the widely recommended approach for correct bootstrap testing [Martin, 2007]. Furthermore, when the parameter lies on the boundary of the parameter space, the classical bootstrap is invalid [Andrews, 2000]. On the other hand, Cavaliere et al. [2017] prove that the *restricted* bootstrap (resampling with the null hypothesis imposed) is consistent even when testing that the parameter is on the boundary. We therefore take $\hat{\theta}_0$, an estimate of θ_0 , as the value which maximizes the log-likelihood derived from the approximate distribution in (10), imposing the constraint given by the null hypothesis. This log-likelihood is proportional to $-\frac{n}{2}(\tilde{\theta}_{n,E} - \theta_{n,E}^*)^\top \tilde{I}_{n,E}(\tilde{\theta}_{n,E} - \theta_{n,E}^*)$,

and we obtain $\hat{\theta}_0$ as

$$\sqrt{n}\hat{\theta}_0 = \underset{\theta}{\operatorname{argmin}} \left\{ \frac{n}{2} (\tilde{\theta}_{n,E} - \theta)^\top \tilde{I}_{n,E} (\tilde{\theta}_{n,E} - \theta) \right\}, \quad \text{s.t. } t(\theta) = t_0.$$

This optimization problem is solved with the R package `nloptr` [Johnson, 2007], using the COBYLA (Constrained Optimization BY Linear Approximations) algorithm [Powell, 1994]. We thus simulate $N = 10^4$ values $\sqrt{n}\theta_0^{(1)}, \dots, \sqrt{n}\theta_0^{(N)}$ from a multivariate normal distribution with mean $\sqrt{n}\hat{\theta}_0$ and covariance matrix $[\tilde{I}_{n,E}]^{-1}$. For each of these observations, we compute $t_0^{(h)} = t(\theta_0^{(h)})$. If the null value we are testing (fixed prior to seeing the data) is 0, we compute the one-sided p-value for the observed value $t(\tilde{\theta}_{n,E})$ as $\#\{t_0^{(h)} \leq t(\tilde{\theta}_{n,E})\}/N$. If $\theta_0 > 0$, we can compute the two-sided p-value as $2 \min\{\#\{t_0^{(h)} \leq t(\tilde{\theta}_{n,E})\}/N, \#\{t_0^{(h)} \geq t(\tilde{\theta}_{n,E})\}/N\}$.

Case (e). The same technique holds to obtain a p-value for bridge strength, using the estimator $\hat{t}_b(\tilde{\theta}_{n,E}) = \sum_{i \in E_j^{(b)}} |\tilde{\theta}_{n,E;i}|$.

Case (g). The test for the difference in node (or bridge) strength between two nodes j and l can be conducted using the test statistic $t_{jl}(\tilde{\theta}_{n,E}) = \sum_{i \in E_j} |\tilde{\theta}_{n,E;i}| - \sum_{i \in E_l} |\tilde{\theta}_{n,E;i}|$ and proceeding in an analogous way.

4.4 Elastic net penalty

When nodes are highly correlated with each other, the variance estimates can become unstable (see Guglielmini and Claeskens [2025] for a toy example of this phenomenon). Similarly to elastic net regression, an additional penalty on the ℓ_2 norm can be applied in the graphical lasso problem. The “graphical elastic net” can be solved with the algorithm in Kovács et al. [2021], which uses coordinate descent in a modified graphical lasso algorithm. The penalty is therefore $\mathcal{P}_\gamma(x) = \lambda_n[\gamma x + \frac{1-\gamma}{2}x^2]$, where $\lambda_n > 0$ and $\gamma \in [0, 1]$. The method for selective inference after elastic net selection is analogous to the one for the lasso selection, with an adjustment to the definition of the randomization map.

Proposition 4. *Define the map $\tilde{\Pi}_{\theta, \theta^\perp} : \mathbb{R}^{|E|} \times \mathbb{R}^d \rightarrow \mathbb{R}^d : (b, u) \mapsto C_1\theta + \tilde{C}_2b + \tilde{f}(u, \theta^\perp)$, where $C_1 = -J_{n,E}J_{n,EE}^{-1}H_{n,EE}$, $K_n = \lambda_n(1 - \gamma)D_p^\top D_p/2$, $\tilde{C}_2 = (H_{n,E} + K_{n,E})\operatorname{diag}(S)$ and*

$\tilde{f}(U; \sqrt{n}\theta_{\perp}) = \gamma \frac{\sqrt{n}}{2} D_p^{\top} \text{vec}(\hat{\mathcal{P}}') + \sqrt{n}\theta_{\perp}$. Then,

$$\sqrt{n}\omega_n = \tilde{\Pi}_{\sqrt{n}\bar{\theta}_{n,E}, \sqrt{n}\bar{\theta}_{\perp}}(\sqrt{n}B, U) + o_P(1).$$

Therefore, when working with the elastic net penalty, the definitions in Proposition 2 should be substituted by the ones in Proposition 4. Note that the adjustments to the matrices only depend on fixed quantities. Proposition 3, Theorems 1 and 2 still hold, with the definitions in Proposition 4.

5 Simulation study

5.1 Settings

Scale-free graph. In the first simulation study, we consider a scale-free graph, with a few highly connected hubs and many nodes with sparse connections, where approximately 10% of the edges are present in the true precision matrix. For the randomized approach, we set $\lambda_n = \sqrt{2 \log(p)/n}$, a choice sometimes referred to as the “universal” penalty level [Sun and Zhang, 2013], while for the non-randomized approach, we set $\lambda_n = \sqrt{\log(p)/n}$. Simulations show that these values lead to similar proportions of selected edges, which allows to fairly compare the selection accuracy across methods. We generate data from a centered and scaled multivariate normal distribution and conduct simulations using both the graphical lasso penalty and the elastic net with $\gamma = 0.5$. Our experiments cover three different settings: a low-dimensional setting with $p = 50$, $n = 1000$ and two high-dimensional ones with $p = 100$, $n = 80$ and $p = 100$, $n = 40$. For each setting, we perform 100 simulation runs and compare the following methods in each run:

1. *Selective inference with randomization (SIR)*: our method for selective inference with randomization;
2. *Data splitting (DS)*: using 50% of the sample for selection and 50% for inference with

the unconditional Gaussian pivot;

3. *Polyhedral without randomization (POLY)*: selective inference with the polyhedral lemma (without randomization) [Guglielmini and Claeskens, 2025];
4. *Naive*: unconditional Gaussian pivot, as if the model were fixed to the selected one.

For each method, we first measure the performance of the initial selection method, to track how the accuracy of selection is affected by randomization and sample splitting: the *F1* score, defined as $F1 = \frac{TP}{TP+(FP+FN)/2}$, where *TP* (True Positives) is the number of true (nonzero) edges which are selected, *FP* (False Positives) the number of true zeroes which are selected, *FN* (False Negatives) the number of true edges which are not selected. This shows that the two randomized methods achieve a similar quality of selection, which is comparable to the non-randomized methods when selecting a similar number of edges.

To evaluate the quality of inference, we compute confidence intervals for all selected edges and measure the simulated coverage as the percentage of times that the target is included in the interval, comparing this with the nominal coverage. The target is $\theta_{n,j}^*$, for $j \in E$: that is, the pseudo-true value, or true value in the selected model. It is obtained in practice by passing the true Θ as input to the constrained optimization problem in Equation (3), where we restrict the elements in E' to be 0. We analogously obtain the coverage for node strength and the two types of expected influence (targets in (b), (c), (d) in Section 2.1), for each node which is connected to at least one selected edge, and for the difference in node strength between two randomly selected, non-isolated nodes.

As a measure of inferential power, we present the average length of the confidence intervals. Especially in larger dimensions, it happens that a small proportion of the elements which are null in the true Θ , but pass the selection step, take a nonzero value in the pseudo-true $\Theta_{n,E}^*$. This is a kind of type I error, we report its rate in the tables as “Target error”.

Modular graph. In the second study, we generate a modular graph (one which presents a community structure, as described in Section 2.1) using the function `sample_islands`

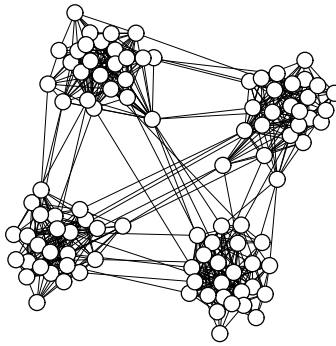


Figure 1: The graph used to generate the data with modular structure.

from the R package `igraph` and adding random weights, with $p = 100$ nodes, divided into 4 subgraphs of size 25, which have higher density of connections within than between them (see Figure 1). We show coverage for the selected edges and for the bridge strength and expected influence (targets in (e) and (f) in Section 2.1), for nodes which are connected to at least one selected bridging edge. We simulate samples of $n = 200$ observations from the modular graph and run 100 simulations.

5.2 Results

Simulation results for the scale-free graph. The results for the scale-free graph under different simulation settings are presented in Tables 1 and 2, where the most relevant comparisons are highlighted in color. Our method outperforms the naive one by displaying coverage that is close to the nominal level (approaching it as the sample size increases), for single edges and for all the composite measures considered, both in the high- and low-dimensional settings. In addition to this, it produces shorter confidence intervals when compared to all other methods with coverage guarantees (DS and POLY). This aligns with expectations, as the polyhedral method without randomization yields excessively long

intervals for the pseudo-true parameters. Our intervals are also substantially shorter than those from the inefficient data-splitting method, which relies solely on holdout samples for inference.

Furthermore, depending on the size and sparsity of the graph and on the penalty level, the sample size needs to be above a certain threshold in order for the Hessian to be invertible. Naturally, since the randomized method utilizes the entire sample size, this threshold is lower than for data splitting. Table 2 (left) shows the results for our method in a setting with $p = 100$ and $n = 40$, where data splitting inference cannot be computed, while randomized selective inference can be conducted for all 100 iterations.

Table 1: Simulated coverage of confidence intervals with nominal coverage 95%; average interval length, F1 score, for dimensions $n = 80, p = 100$ and $n = 1000, p = 50$; on multivariate normal data with scale-free structure, after graphical lasso selection, randomization $\text{st.dev} = 1$.

	$n = 80, p = 100$				$n = 1000, p = 50$			
	SIR	DS	POLY	Naive	SIR	DS	POLY	Naive
F1	0.109	0.110	0.175	0.175	0.575	0.580	0.621	0.621
Target error	0.023	0.023	0.022	0.022	0.019	0.018	0.012	0.012
95% cov. (a)	0.939	0.960	0.959	0.228	0.955	0.950	0.942	0.569
Int. length (a)	0.589	0.718	Inf	0.438	0.157	0.184	Inf	0.125
95% cov. (b)	0.941	0.951	-	0.045	0.961	0.952	-	0.429
95% cov. (c)	0.940	0.950	-	0.561	0.950	0.959	-	0.672
Int. length (c)	1.090	1.337	-	0.834	0.325	0.375	-	0.263
95% cov. (d)	0.955	0.967	-	0.614	0.946	0.953	-	0.655
Int. length (d)	1.214	1.592	-	1.069	0.338	0.392	-	0.269
95% cov. (g)	0.966	0.973	-	0.648	0.961	0.962	-	0.730

Table 2: Simulated coverage of confidence intervals with nominal coverage 95%; average interval length, F1 score; on multivariate normal data with scale-free structure, after graphical lasso (high dimensional case) and elastic net selection, randomization st.dev = 1.

	Graph. lasso ($n = 40, p = 100$)			Elastic net ($n = 1000, p = 50$)			
	SIR	POLY	Naive	SIR	DS	POLY	Naive
F1	0.072	0.103	0.103	0.573	0.577	0.616	0.616
Target error	0.023	0.022	0.022	0.019	0.019	0.013	0.013
95% cov. (a)	0.938	0.961	0.175	0.957	0.950	0.937	0.570
Int. length (a)	0.866	Inf	0.620	0.160	0.184	Inf	0.125
95% cov. (b)	0.927	-	0.035	0.961	0.952	-	0.433
95% cov. (c)	0.921	-	0.540	0.953	0.959	-	0.673
Int. length (c)	1.568	-	1.134	0.333	0.377	-	0.265
95% cov. (d)	0.958	-	0.620	0.950	0.955	-	0.646
Int. length (d)	1.979	-	1.677	0.347	0.395	-	0.270
95% cov. (g)	0.956	-	0.663	0.960	0.960	-	0.729

Simulation results 2 for the modular graph. Table 3 displays the coverage and average interval length of the confidence intervals for bridge strength and expected influence, computed for the modular graph, for our randomized method (SIR), data splitting (DS) and the naive method.

6 Data application

We now consider an application of our method to cortical thickness data, measured via magnetic resonance imaging (MRI), from $n = 59$ healthy subjects in the OASIS-1 dataset [Marcus et al., 2007]. Pre-processed data, using the software FreeSurfer, were provided by OASIS (Open Access Series of Imaging Studies). The resulting dataset consists of

Table 3: Simulated coverage of confidence intervals of bridge centrality measures with nominal coverage 95%; average interval length, F1 score, with $n = 200$, $p = 100$; on multivariate normal data with modular structure, after graphical lasso selection, randomization st.dev = 1.

Modular Graph ($n = 200, p = 100$)			
	SIR	DS	Naive
F1	0.138	0.142	0.229
Target error	0.019	0.018	0.018
95% cov. (e)	0.950	0.951	0.042
95% cov. (f)	0.944	0.947	0.434
Int. length (f)	0.586	0.662	0.437

$p = 66$ brain regions, parcellated according to the Desikan-Killiany atlas [Desikan et al., 2006] (excluding the *corpus callosum*). We therefore model the data with a structural connectivity network and select the edges using the randomized graphical lasso, with $\lambda_n = \sqrt{2 \log(p)/n}$ and standard deviation of the randomization variable equal to 1. The selected graph is displayed in Figure 2.

As introduced in Section 2.1, we consider inference on measures of influence and integration. Focusing on measures of influence, we consider the centrality ranking of the regions as proposed by Chen et al. [2008] (based on independently collected data). We test the null hypothesis that the node strength of the left precentral gyrus (the most central node in the proposed ranking) is not significantly different from that of the right parahippocampal gyrus (below average centrality). On the OASIS data, we indeed estimate the node strength for the left precentral gyrus as 16.999, higher than the one for the parahippocampal gyrus (2.559). The p-value of the test is $2 \cdot 10^{-4}$, indicating a significant difference between the strength centrality of the two nodes. We repeat the analysis for the expected influence

(estimated for the two nodes as -6.195 and -1.002 respectively), and obtain a p-value equal to 0.002, which also leads us to reject the null hypothesis, confirming the findings in Chen et al. [2008]. For an analysis of an integration measure, we consider 5 modules, according to the anatomical structure of the cortex: the modules are defined as the frontal, parietal, temporal, occipital and cingulate lobes. We then test the difference in bridge strength between the left precuneus, a region which has been found to be functionally connected to other regions of the brain [Margulies et al., 2009], and the left pericalcarine, a region associated with the primary visual cortex, which tends to have stronger local functional connectivity, rather than global [Sepulcre et al., 2010]. While functional connectivity and structural connectivity are different concepts, there is often a considerable correlation between the two [Greicius et al., 2009]. We therefore expect the precuneus and the pericalcarine to also present a significant difference in bridge strength in the MRI data. Indeed, the bridge strength is estimated for the left precuneus as 3.509 and for the left pericalcarine as 0.684, and the p-value of the significance test for this difference is 0.026, allowing us to reject the null hypothesis at a 5% confidence level. As for the bridge expected influence, the left precuneus presents an estimate of 2.797 and the left pericalcarine one of 0.684, giving a p-value for the significance test of the difference equal to 0.004, which again allows us to reject the null hypothesis of equal bridge influence in the two regions. The results we obtained using our randomized method on the OASIS data are thus in line with the previous literature on brain connectivity. The results are summarized in Table 4 in the online Appendix.

We further show, in the right panel of Figure 2, the graph containing only the edges which are found to be significant at a confidence level of 95%, after conducting randomized selective inference on each selected edge.

A Extra tables

	Strength	Exp. influence
PrCG.L	16.999	-6.195
PHG.R	2.559	-1.002
Significance	$2 \cdot 10^{-4}$	0.002

	Bridge strength	Bridge exp. influence
PCU.L	3.509	2.797
PCal.L	0.684	0.684
Significance	0.026	0.004

Table 4: Summary of results of the data application in Section 6. The data consists of MRI measurements of the cortical thickness of $p = 66$ brain regions on $n = 56$ healthy subjects, provided by OASIS [Marcus et al., 2007]. For the two pairs of regions (PrCG.L, left precentral gyrus and PHG.R, right parahippocampal gyrus; PCU.L, left precuneus and PCal.L, left pericalcarine), the estimates of centrality and the p-value of the significance test for the difference in centrality, are displayed.

Quantity	Value
ω_n	ω/\sqrt{n}
D_p	duplication matrix of order p
H_n	$D_p^\top(\bar{\Sigma} \otimes \bar{\Sigma})D_p$
J_n	$\sum_{h=1}^n [D_p^\top \text{vec}(-\bar{\Sigma} + X_h X_h^\top) \text{vec}(-\bar{\Sigma} + X_h X_h^\top)^\top D_p] / 4n$
E	$\{j : \text{vh}(\hat{\Theta})_j \neq 0\}$
E'	$\{j : \text{vh}(\hat{\Theta})_j = 0\}$
Σ_E	$H_{n,E'E}^{-1} J_{n,E'E} H_{n,EE}^{-1}$
$\bar{\theta}$	$\text{vh}(\bar{\Theta})$
$\bar{\Sigma}$	$\bar{\Theta}^{-1}$
A_E	$H_{n,E'E} - J_{n,E'E} J_{n,EE}^{-1} H_{n,EE}$
$\theta_{E'}^\perp$	$D_p^\top \text{vec}(-\bar{\Sigma} + S_n) / 2 - A_E \bar{\theta}_E$
θ_E^\perp	$0_{ E }$
C_1	$-J_{n,E} J_{n,EE}^{-1} H_{n,EE}$
C_2	$H_{n,E} \text{diag}(\text{sign}(\text{vh}(\hat{\Theta})_E))$
ℓ'	$D_p^\top \text{vec}(-\hat{\Sigma} + S_n) / 2$
f_u	$\text{subgrad} + \theta^\perp$
Δ	$(C_2^\top \Omega^{-1} C_2)^{-1}$
P	$-\Delta C_2^\top \Omega^{-1} C_1$
q	$-\Delta C_2^\top \Omega^{-1} f_u$
Z	$(\Sigma_E^{-1} - P^\top \Delta^{-1} P + C_1^\top \Omega^{-1} f_u)^{-1}$
L	$Z \Sigma_E^{-1}$
m	$Z P^\top \Delta^{-1} q - C_1^\top \Omega^{-1} f_u$

Table 5: Quantities for Algorithm 1

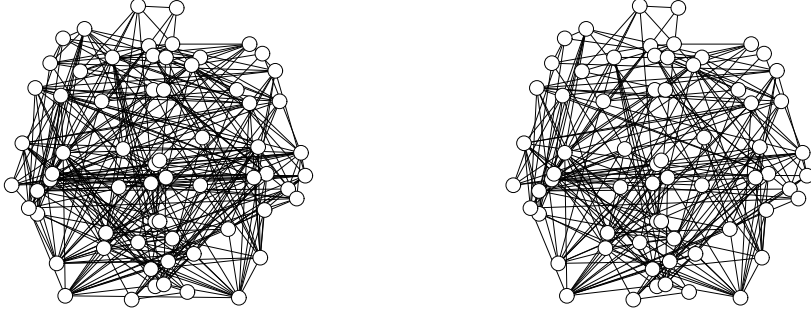


Figure 2: The selected graph (left) and the one with significant edges only (right) for the OASIS-1 cortical thickness dataset. The nodes are positioned in the display based on the location of the corresponding cortex region in the human brain, according to the coordinates provided in the dataset `dk` in the R package `brainGraph`.

B Probabilistic justification for the Laplace approximation

We obtain the limit for the probability in the denominator of the conditional likelihood in Equation (8).

By Equations (13) and (14), we can write

$$\sqrt{n}((\bar{\theta}_{n,E} - \theta_{n,E}^*)^\top, (\bar{\theta}_{n,E}^\perp - \theta_{n,E}^{\perp*})^\top, \bar{\omega}_n^\top)^\top = T\sqrt{n}\bar{Z}_n + \bar{r}_n,$$

where $\bar{r}_n = o_P(1)$, $\bar{Z}_n = n^{-1} \sum_{i=1}^n Z_{n,i}$ is the mean of n i.i.d. observations, and

$$T = \begin{pmatrix} -H_{n,EE}^{-1} & 0_{|E|,|E'|} & 0_{|E|,d} \\ H_{n,E'E} - A_E & I_{|E|} & 0_{|E'|,d} \\ 0_{d,|E|} & 0_{d,|E'|} & I_d \end{pmatrix}$$

is an invertible matrix and its entries asymptotically converge to fixed values. Observe that $T\sqrt{n}\bar{Z}_n \xrightarrow{d} N_{2d}(0_{2d}, \text{diag}(\Sigma_E, \Sigma_E^\perp, \Omega))$.

Assumption 2 (Moment condition and convergence of remainder, see Assumption 3.2 in Huang et al. [2023a]). *Assume that $\mathbb{E}[\exp(\delta\|Z_{n,1}\|_2)] < \infty$ for some $\delta \in \mathbb{R}^+$, and that for*

a sequence with $a_n = o(\sqrt{n})$ and $a_n \rightarrow \infty$, for any $\epsilon > 0$

$$\lim_{n \rightarrow \infty} \frac{1}{a_n^2} \log \mathbb{P} \left[\frac{1}{a_n} \|\bar{r}_n\|_2 > \epsilon \right] = -\infty.$$

Assumption 3 (See Assumption 3.3 in Huang et al. [2023a]). Let $\mathcal{R} \subseteq \mathbb{R}^{2d}$ be a convex set and for any sequence of random variables C_n with bounded support, for any $\epsilon > 0$, $a_n = o(\sqrt{n})$ and $a_n \rightarrow \infty$ as $n \rightarrow \infty$,

$$\lim_{n \rightarrow \infty} \frac{1}{a_n} \left\{ \log \mathbb{P} \left[\frac{\sqrt{n}}{a_n} \bar{Z}_n \in \mathcal{R} \right] - \log \mathbb{P} \left[\frac{\sqrt{n}}{a_n} \bar{Z}_n + \frac{C_n}{a_n} \in \mathcal{R} \right] \right\} = 0.$$

Define the barrier function which enforces the linear constraints $\nu_h > c$.

$$\phi(\nu) = - \sum_{h=1}^{|\nu|} \log(\nu_h - c).$$

Theorem 3 (Theorem 3.2 in Huang et al. [2023a]). Denote $\mathcal{K} = [c, \infty]^{|E|}$ and suppose $\sqrt{n}\theta_{n,E}^* = a_n\theta_{n,E}$, where $a_n = o_P(\sqrt{n})$. Let

$$\begin{aligned} O_n = & - \inf_{\tilde{\theta}, \tilde{b}} \left\{ \frac{1}{2} (\tilde{\theta} - L\theta_{n,E}^* - a_n^{-1}m)^\top Z^{-1} (\tilde{\theta} - L\theta_{n,E}^* - a_n^{-1}m) \right. \\ & \left. + \frac{1}{2} (\tilde{b} - P\tilde{\theta} - a_n^{-1}q)^\top \Delta^{-1} (\tilde{b} - P\tilde{\theta} - a_n^{-1}q) + a_n^{-2} \phi_{\mathcal{K}}(a_n \tilde{b}) \right\}. \end{aligned}$$

Under the assumptions above,

$$\lim_{n \rightarrow \infty} \frac{1}{a_n^2} \log \mathbb{P}[\sqrt{n}B \in \mathcal{K} \mid \bar{\theta}_\perp = \theta_\perp^*, \hat{S} = S, \hat{U} = U] - O_n \rightarrow 0.$$

Therefore, due to this Theorem, we can substitute

$$\log \mathbb{P}[\sqrt{n}B \in \mathcal{K} \mid \bar{\theta}_\perp = \theta_\perp^*, \hat{S} = S, \hat{U} = U]$$

with the optimization

$$\begin{aligned} a_n^2 O_n = & - \inf_{\tilde{\theta}, \tilde{b}} \left\{ \frac{1}{2} (a_n \tilde{\theta} - L\sqrt{n}\theta_{n,E}^* - m)^\top Z^{-1} (a_n \tilde{\theta} - L\sqrt{n}\theta_{n,E}^* - m) \right. \\ & \left. + \frac{1}{2} (a_n \tilde{b} - Pa_n \tilde{\theta} - q)^\top \Delta^{-1} (a_n \tilde{b} - Pa_n \tilde{\theta} - q) + \phi_{\mathcal{K}}(a_n \tilde{b}) \right\}, \end{aligned}$$

where $\mathcal{K} = [c, \infty]^{|E|}$. We take $c = 0$ or close to 0, $a_n \tilde{\theta} = \sqrt{n}\theta$ and $a_n \tilde{b} = \sqrt{n}b$.

C Lemma's and proofs

Lemma 4. Consider $\sqrt{n}X \sim N(\mu, V)$, an arbitrary set E and an estimator with the form $\sum_{i \in E} |X_i|$. Then the estimator is \sqrt{n} -bounded, that is, $\sqrt{n}(\sum_{i \in E} |X_i| - \sum_{i \in E} |\mu_i|) = O_P(1)$.

Proof of Lemma 4. We now analyze the consistency of the estimator of the node and bridge strength. If all elements of $\theta_{n,E_j}^* \neq 0$, $t(\tilde{\theta}_{n,E})$ is a consistent estimator of $t(\theta_{n,E}^*)$. Indeed, for $\sqrt{n}X \sim N(\mu, V)$ and an arbitrary set E , using the expectation of the folded normal distribution [Leone et al., 1961]

$$\sqrt{n}\mathbb{E} \left[\sum_{i \in E} |X_i| \right] = \sum_{i \in E} \mathbb{E} [|\sqrt{n}X_i|] = \sum_{i \in E} \left(\sqrt{\frac{2V_{ii}}{\pi}} e^{-\frac{n\mu_i^2}{2V_{ii}}} + \sqrt{n}\mu_i \left[1 - 2\Phi \left(\frac{-\sqrt{n}\mu_i}{\sqrt{V_{ii}}} \right) \right] \right).$$

If $\mu_i \neq 0$, as $n \rightarrow \infty$,

$$\sqrt{n}\mathbb{E} \left[\sum_{i \in E} |X_i| \right] \rightarrow \begin{cases} 0 + \sqrt{n}\mu_i \times 1 & \text{if } \mu_i > 0 \\ 0 + \sqrt{n}\mu_i \times (-1) & \text{if } \mu_i < 0, \end{cases}$$

therefore

$$\sqrt{n}\mathbb{E} \left[\sum_{i \in E} |X_i| \right] \rightarrow \sum_{i \in E} |\mu_i|.$$

If $\mu_i = 0$, it adds the bias term

$$\sqrt{\frac{2V_{ii}}{\pi}}.$$

Note that, if we work in the scale of X instead of $\sqrt{n}X$, then the standard deviation is itself $O_P(n^{-1/2})$, and so is the bias. The estimator is thus \sqrt{n} -bounded and the bias does not diverge with n . The simulated null distribution for the bootstrap p-value correctly reflects how the test statistic is distributed under the null (including the shift for zero means), without need for bias correction. \square

Proof of Lemma 2. We first prove that $H_{n,EE}(\hat{\Theta}_{n,E})$, the submatrix of $H_n(\hat{\Theta}_{n,E})$ is positive definite. $H_n(\Theta)$ is defined as [Guglielmini and Claeskens, 2025]

$$H_n(\Theta) = n^{-1} \sum_{h=1}^n \frac{\partial^2 \ell_n(\Theta, X_h)}{\partial \text{vh}(\Theta) \partial \text{vh}(\Theta)^\top} = \frac{1}{2} D_p^\top (\Theta^{-1} \otimes \Theta^{-1}) D_p,$$

If $\widehat{\Theta}_{n,E}$ is positive definite, then so is $\widehat{\Theta}_{n,E}^{-1}$. By Van Loan and Pitsianis [1993], $\widehat{\Theta}_{n,E}^{-1} \otimes \widehat{\Theta}_{n,E}^{-1}$ is thus positive definite.

The duplication matrix has full column rank [Equation (4.4) in Harville, 1998], therefore, by Theorem 14.2.9 in Harville [1998],

$$D_p^\top (\widehat{\Theta}_{n,E}^{-1} \otimes \widehat{\Theta}_{n,E}^{-1}) D_p$$

is positive definite. Noting that multiplication by a scalar does not affect positive-definiteness, this proves that $H_n(\widehat{\Theta}_{n,E})$ is positive definite.

By simultaneously interchanging rows and columns of $H_n(\widehat{\Theta}_{n,E})$ so that the rows and columns indexed by E come first, positive definiteness is not affected and $H_{n,EE}(\widehat{\Theta}_{n,E})$ can then be represented as a principal submatrix of $H_n(\widehat{\Theta}_{n,E})$. Therefore, by Corollary 14.2.12 in Harville [1998], $H_{n,EE}(\widehat{\Theta}_{n,E})$ is also positive definite.

Let us now consider the case where $n \geq d$. $J_{n,EE}(\widehat{\Theta}_{n,E})$ is a submatrix of $J_n(\widehat{\Theta}_{n,E})$, defined as [Guglielmini and Claeskens, 2025]:

$$J_n(\Theta) = n^{-1} \sum_{h=1}^n [G(\Theta; X_h)^\top G(\Theta; X_h)],$$

where G is the $1 \times d$ vector

$$G(\Theta; X_h) = \frac{\partial \ell_n(\Theta; X_h)}{\partial \text{vh}(\Theta)^\top} = \frac{1}{2} \text{vec}(-\Theta^{-1} + X_h X_h^\top)^\top D_p.$$

Define G_n as the $n \times d$ matrix in which the h -th row is $G(\Theta; X_h)$. Note that $J_n(\widehat{\Theta}_{n,E})$ can then be expressed as $n^{-1} G_n^\top G_n$.

X_1, \dots, X_n are independent observations, and $G(\Theta; X_h)$ is a linear function of X_h (the $\text{vec}(\cdot)$ operator and the duplication matrix are linear operators). Then G_n has $\min(n, d)$ linearly independent rows, thus $\text{rank}(G_n) = \min(n, d)$. By Corollary 14.2.14 in Harville [1998], $G_n^\top G_n$ is positive definite if $\text{rank}(G_n) = d$. This is true if $n \geq d$, and in this case $J_n(\widehat{\Theta}_{n,E})$ is positive definite and, analogously to the first part of the proof, also its submatrix $J_{n,EE}(\widehat{\Theta}_{n,E})$.

To prove that $J_{n,EE}(\widehat{\Theta}_{n,E})$ is positive definite in the case $|E| \leq n < d$ (although $J_n(\widehat{\Theta}_{n,E})$ is not), we first define the $n \times |E|$ matrix $G_{n,E}$ as the set of columns of G_n indexed by E . Then

$$J_{n,EE}(\widehat{\Theta}_{n,E}) = n^{-1}G_{n,E}^\top G_{n,E}.$$

Analogously to the previous case, $\text{rank}(G_{n,E}) = \min(n, |E|) = |E|$, thus $G_{n,E}^\top G_{n,E}$, and therefore $J_{n,EE}(\widehat{\Theta}_{n,E})$, is positive definite. □

Proof of Proposition 1. Assuming without loss of generality that the elements with index in E come before the ones with index in E' , take the first $|E|$ rows of the Taylor series expansion of the gradient evaluated at the refitted estimator $\bar{\theta}_{n,E}$ around the true value $\theta_{n,E}^*$. By definition of the refitted estimator,

$$n^{-1/2} \frac{\partial \ell_n(\bar{\Theta}_{n,E}; X)}{\partial \text{vh}(\Theta)_E} = 0_{|E|}.$$

Since

$$n^{-1/2} \frac{\partial \ell_n(\bar{\Theta}_{n,E}; X)}{\partial \text{vh}(\Theta)_E} = n^{-1/2} \frac{\partial \ell_n(\Theta_{n,E}^*; X)}{\partial \text{vh}(\Theta)_E} + H_{n,EE} \sqrt{n}(\bar{\theta}_{n,E} - \theta_{n,E}^*) + o_P(1) = 0_{|E|},$$

then

$$\sqrt{n}(\bar{\theta}_{n,E} - \theta_{n,E}^*) = -H_{n,EE}^{-1} n^{-1/2} \frac{\partial \ell_n(\Theta_{n,E}^*; X)}{\partial \text{vh}(\Theta)_E} + o_P(1). \quad (13)$$

By the asymptotic properties of M -estimators [Huber, 1981],

$$J_{n,E'E'}^{-1/2} n^{-1/2} \left\{ \frac{\partial \ell_n(\Theta_{n,E}^*; X)}{\partial \text{vh}(\Theta)_{E'}} - \mathbb{E} \left[\frac{\partial \ell_n(\Theta_{n,E}^*; X)}{\partial \text{vh}(\Theta)_{E'}} \right] \right\} \xrightarrow{d} N_{|E'|}(0_{|E'|}, I_{E'}).$$

Using this result for the variance, the proof is complete. □

Proof of Lemma 3. We want to define a vector that is orthogonal with respect to the parameters in the selected model indexed by E . Take the last $|E'|$ rows of the Taylor series expansion of the gradient evaluated at the refitted estimator around the pseudo-true value:

$$n^{-1/2} \frac{\partial \ell_n(\bar{\Theta}_{n,E}; X)}{\partial \text{vh}(\Theta)_{E'}} = n^{-1/2} \frac{\partial \ell_n(\Theta_{n,E}^*; X)}{\partial \text{vh}(\Theta)_{E'}} + H_{n,E'E} \sqrt{n}(\bar{\theta}_{n,E} - \theta_{n,E}^*) + o_P(1).$$

Insert this expression in the definition of $\bar{\theta}_{n,E}^\perp$,

$$\bar{\theta}_{n,E}^\perp = n^{-1} \frac{\partial \ell_n(\Theta_{n,E}^*; X)}{\partial \text{vh}(\Theta)_{E'}} + H_{n,E'E}(\bar{\theta}_{n,E} - \theta_{n,E}^*) - A_E \bar{\theta}_{n,E} + o_P(1).$$

Hence

$$\sqrt{n}(\bar{\theta}_{n,E}^\perp - \theta_{n,E}^{\perp,*}) = (H_{n,E'E} - A_E) \sqrt{n}(\bar{\theta}_{n,E} - \theta_{n,E}^*) + n^{-1/2} \left\{ \frac{\partial \ell_n(\Theta_{n,E}^*; X)}{\partial \text{vh}(\Theta)_{E'}} - \mathbb{E} \left[\frac{\partial \ell_n(\Theta_{n,E}^*; X)}{\partial \text{vh}(\Theta)_{E'}} \right] \right\} + o_P(1). \quad (14)$$

The variance of the first term is

$$\begin{aligned} \text{Var}\{(H_{n,E'E} - A_E) \sqrt{n}(\bar{\theta}_{n,E} - \theta_{n,E}^*)\} &= J_{n,E'E} J_{n,EE}^{-1} H_{n,EE} \Sigma_E (J_{n,E'E} J_{n,EE}^{-1} H_{n,EE})^\top \\ &= J_{n,E'E} J_{n,EE}^{-1} H_{n,EE} [H_{n,EE}^{-1} J_{n,EE} H_{n,EE}^{-1}] H_{n,EE} J_{n,EE}^{-1} J_{n,EE}' \\ &= J_{n,E'E} J_{n,EE}^{-1} J_{n,EE}'. \end{aligned}$$

Now, rewriting the first term on the right-hand side of (14) using the result in (13), the covariance between this term and the second term in (14) is

$$\begin{aligned} &-(H_{n,E'E} - A_E) H_{n,EE}^{-1} \text{Cov} \left(n^{-1/2} \frac{\partial \ell_n(\Theta_{n,E}^*; X)}{\partial \text{vh}(\Theta)_E}, n^{-1/2} \frac{\partial \ell_n(\Theta_{n,E}^*; X)}{\partial \text{vh}(\Theta)_{E'}} \right) \\ &= -(H_{n,E'E} - A_E) H_{n,EE}^{-1} J_{n,EE}' = -J_{n,E'E} J_{n,EE}^{-1} J_{n,EE}'. \end{aligned} \quad (15)$$

Furthermore, by the central limit theorem,

$$J_{n,E'E}^{-1/2} n^{-1/2} \left\{ \frac{\partial \ell_n(\Theta_{n,E}^*; X)}{\partial \text{vh}(\Theta)_{E'}} - \mathbb{E} \left[\frac{\partial \ell_n(\Theta_{n,E}^*; X)}{\partial \text{vh}(\Theta)_{E'}} \right] \right\} \xrightarrow{d} N_{|E'|}(0_{|E'|}, I_{E'}).$$

Using these results and Proposition 1, then

$$\sqrt{n}(\bar{\theta}_{n,E}^\perp - \theta_{n,E}^{\perp,*}) \xrightarrow{d} N_{|E'|}(0_{|E'|}, \Sigma_{E^\perp}),$$

where $\Sigma_{E^\perp} = J_{n,E'E} - J_{n,E'E} J_{n,EE}^{-1} J_{n,EE}'$. By construction, $\bar{\theta}_{n,E}^\perp$ is orthogonal to $\bar{\theta}_{n,E}$. Indeed,

using (14) and (15),

$$\begin{aligned}
& \text{Cov} \left\{ \sqrt{n}(\bar{\theta}_{n,E} - \theta_{n,E}^*), \sqrt{n}(\bar{\theta}_{n,E}^\perp - \theta_{n,E}^{*\perp}) \right\} \\
&= \Sigma_E (H_{nE'E} - A_E)^\top - H_{nEE}^{-1} J_{n,EE'} \\
&= (H_{n,EE}^{-1} J_{n,EE} H_{n,EE}^{-1}) (J_{n,E'E} J_{n,EE}^{-1} H_{n,EE})^\top - H_{nEE}^{-1} J_{n,EE'} \\
&= H_{n,EE}^{-1} J_{n,EE} H_{n,EE}^{-1} H_{n,EE} J_{n,EE}^{-1} J_{n,EE'} - H_{nEE}^{-1} J_{n,EE'} \\
&= H_{nEE}^{-1} J_{n,EE'} - H_{nEE}^{-1} J_{n,EE'} = 0_{|E|,|E'|}.
\end{aligned}$$

Under asymptotic normality, zero covariance implies independence and the proof is complete. \square

Proof of Proposition 2. By the Karush-Kuhn-Tucker conditions of the optimization problem in (2)

$$\begin{aligned}
& \frac{\partial}{\partial \text{vh}(\Theta)} \left\{ \text{tr}((S_n - W_n)\Theta) - \log \det(\Theta) + \lambda_n \|\Theta\|_1 \right\} \Big|_{\Theta = \hat{\Theta}_{n,\lambda_n}} = 0 \\
& D_p^\top \text{vec}(S_n - W_n - \hat{\Theta}_{n,\lambda_n}^{-1} + \hat{\mathcal{P}}') = 0 \\
& \frac{\sqrt{n}}{2} D_p^\top \text{vec}(S_n - \hat{\Theta}_{n,\lambda_n}^{-1}) - \frac{\sqrt{n}}{2} D_p^\top \text{vec}(W_n) + \frac{\sqrt{n}}{2} D_p^\top \text{vec}(\hat{\mathcal{P}}') = 0, \\
& n^{-1/2} \frac{\partial \ell_n(\hat{\Theta}_{n,\lambda_n}; X)}{\partial \text{vh}(\Theta)} - \sqrt{n} \omega_n + \frac{\sqrt{n}}{2} D_p^\top \text{vec}(\hat{\mathcal{P}}') = 0.
\end{aligned}$$

Now take a Taylor series expansion of the gradient evaluated at the regularized estimator around the refitted estimator:

$$n^{-1/2} \frac{\partial \ell_n(\hat{\Theta}_{n,\lambda_n}; X)}{\partial \text{vh}(\Theta)} = n^{-1/2} \frac{\partial \ell_n(\bar{\Theta}_{n,E}; X)}{\partial \text{vh}(\Theta)} + H_{n,E} \sqrt{n} (\hat{\theta}_{n,\lambda_n} - \bar{\theta}_{n,E}) + o_P(1).$$

Then, using the definition of the orthogonal nuisance vector, and the fact that

$$\hat{\theta}_{n,\lambda_n}(E) = \text{diag}(S)B,$$

we can rewrite the Karush-Kuhn-Tucker conditions as

$$\begin{aligned}
\sqrt{n} \omega_n &= (-J_{n,E} J_{n,EE}^{-1} H_{n,EE}) \sqrt{n} \bar{\theta}_{n,E} + H_{n,E} \sqrt{n} \text{diag}(S)B + \sqrt{n} \bar{\theta}_\perp + \frac{\sqrt{n}}{2} D_p^\top \text{vec}(\mathcal{P}') \\
&= C_1 \sqrt{n} \bar{\theta}_{n,E} + C_2 \sqrt{n} B + f(U; \sqrt{n} \bar{\theta}_\perp).
\end{aligned}$$

\square

Proof of Proposition 3. Consider the mapping

$$\Pi^* : \mathbb{R}^{|E|} \times \mathbb{R}^d \times \mathbb{R}^d \rightarrow \mathbb{R}^{|E|} \times \mathbb{R}^d \times \mathbb{R}^d : (\theta, \theta^\perp, \omega) \rightarrow (\theta, \theta^\perp, \Pi_{\theta, \theta^\perp}^{-1}(\omega)),$$

where

$$\Pi_{\theta, \theta^\perp}^{-1}(\omega) = (B^\top, U^\top)^\top.$$

Denote by \bar{g}_n the density of

$$\sqrt{n}(\bar{\theta}_{n,E}^\top, (\bar{\theta}_{n,E}^\perp)^\top, \bar{\omega}_n^\top)^\top. \quad (16)$$

Then apply Π^* as a change of variables from the vector in (16) to

$$(\sqrt{n}\bar{\theta}_{n,E}^\top, (\sqrt{n}\bar{\theta}_{n,E}^\perp)^\top, \sqrt{n}B^\top, U^\top)^\top,$$

which, by the properties of the transformation of variables, has density function

$$|\det D_{(\Pi^*)^{-1}}|(\sqrt{n}\theta_{n,E}, \sqrt{n}\theta_{n,E}^\perp, \sqrt{n}B, U)|\bar{g}_n(\sqrt{n}\theta_{n,E}, \sqrt{n}\theta_{n,E}^\perp, \Pi_{\sqrt{n}\theta_{n,E}, \sqrt{n}\theta_{n,E}^\perp}(\sqrt{n}B, U)).$$

Note that this density is equivalent to g_n after undoing the centering:

$$\bar{g}_n(\sqrt{n}\theta_{n,E}, \sqrt{n}\theta_{n,E}^\perp, \sqrt{n}\bar{\omega}_n) = g_n(\sqrt{n}(\theta_{n,E} - \theta_{n,E}^*), \sqrt{n}(\theta_{n,E}^\perp - \theta_{n,E}^{\perp*}), \sqrt{n}\bar{\omega}_n).$$

Therefore (C) is equal to

$$|\det D_{(\Pi^*)^{-1}}|(\sqrt{n}\theta_{n,E}, \sqrt{n}\theta_{n,E}^\perp, \sqrt{n}B, U)|g_n(\sqrt{n}(\theta_{n,E} - \theta_{n,E}^*), \sqrt{n}(\theta_{n,E}^\perp - \theta_{n,E}^{\perp*}), \Pi_{\sqrt{n}\theta_{n,E}, \sqrt{n}\theta_{n,E}^\perp}(\sqrt{n}B, U)).$$

Now note that

$$\det D_{\Pi^*}(\theta, \theta^\perp, b, u) = \det \begin{pmatrix} I_{|E|} & 0_{|E|,d} & 0_{|E|,d} \\ 0_{d,|E|} & I_d & 0_{d,d} \\ \frac{\partial \Pi_{\theta, \theta^\perp}^{-1}(\omega)}{\partial \theta} & \frac{\partial \Pi_{\theta, \theta^\perp}^{-1}(\omega)}{\partial \theta^\perp} & \frac{\partial \Pi_{\theta, \theta^\perp}^{-1}(\omega)}{\partial \omega} \end{pmatrix} = \det \left(\frac{\partial \Pi_{\theta, \theta^\perp}^{-1}(\omega)}{\partial \omega} \right) = \frac{1}{\det \left(\frac{\partial \Pi_{\theta, \theta^\perp}(b, u)}{\partial (b, u)} \right)}.$$

Now denote the rows of $\Pi_{\theta, \theta^\perp}(\cdot)$ with indices in E as $\Pi_{\theta, \theta^\perp}^{(E)}(\cdot)$ and the rows with indices in E' as $\Pi_{\theta, \theta^\perp}^{(E')}(\cdot)$. From the definition in (2),

$$\Pi_{\theta, \theta^\perp}^{(E)}(b, u) = -H_{n,EE}\theta + H_{n,EE}\text{diag}(S)b + \sqrt{n}\lambda_n s;$$

$$\Pi_{\theta, \theta^\perp}^{(E')}(b, u) = -J_{n,E'E}J_{n,EE}^{-1}H_{n,EE}\theta + H_{n,E'E}\text{diag}(S)b + \sqrt{n}\lambda_n u + \sqrt{n}\theta^\perp.$$

Now compute $|\det\left(\frac{\partial\Pi_{\theta,\theta^\perp}(\sqrt{n}B,U)}{\partial(\sqrt{n}B,U)}\right)|$ as

$$\begin{aligned} \left|\det\left(\frac{\partial\Pi_{\theta,\theta^\perp}(\sqrt{n}B,U)}{\partial(\sqrt{n}B,U)}\right)\right| &= \left|\det\begin{pmatrix} \frac{\partial\Pi_E}{\partial\sqrt{n}B} & \frac{\partial\Pi_E}{\partial U} \\ \frac{\partial\Pi_{E'}}{\partial\sqrt{n}B} & \frac{\partial\Pi_{E'}}{\partial U} \end{pmatrix}\right| = \left|\det\begin{pmatrix} H_{n,EE}\text{diag}(S) & 0 \\ H_{n,E'E}\text{diag}(S) & \sqrt{n}\lambda_n \end{pmatrix}\right| \\ &= |\det(H_{n,EE}\text{diag}(S)) \det(\sqrt{n}\lambda_n)| = \sqrt{n}\lambda_n |\det(\text{diag}(S))| |\det(H_{n,EE})| \\ &= \sqrt{n}\lambda_n |\det(H_{n,EE})|, \end{aligned}$$

using the fact that $\det(\text{diag}(S)) = \pm 1$. Note that the Jacobian is a constant and does not depend on the parameters $\theta, \theta^\perp, B, U$, thus it is proportional to 1. Naturally, its reciprocal is also proportional to 1, which completes the proof. \square

Proof of Theorem 1. Starting from the density after the change of variables and conditioning on the selection event:

$$\begin{aligned} &\frac{\rho(\sqrt{n}\bar{\theta}_{n,E}; \sqrt{n}\theta_{n,E}^*, \Sigma_E) \rho(\sqrt{n}\bar{\theta}_\perp; \sqrt{n}\theta_\perp^*, \Sigma_\perp^E) \rho(\Pi(\sqrt{n}B, U); 0_d, \Omega) \mathbb{1}_{\mathbb{R}_+^{|E|}}(\sqrt{n}B)}{\int \rho(\sqrt{n}\tilde{\theta}; \sqrt{n}\theta_{n,E}^*, \Sigma_E) \rho(\sqrt{n}\tilde{\theta}_\perp; \sqrt{n}\theta_\perp^*, \Sigma_\perp^E) \rho(\Pi(\sqrt{n}\tilde{B}, U); 0_d, \Omega) \mathbb{1}_{\mathbb{R}_+^{|E|}}(\sqrt{n}\tilde{B}) d\tilde{\theta} d\tilde{B}} \\ &= \frac{\rho(\sqrt{n}\bar{\theta}_{n,E}; \sqrt{n}\theta_{n,E}^*, \Sigma_E) \rho(\Pi(\sqrt{n}B, U); 0_d, \Omega) \mathbb{1}_{\mathbb{R}_+^{|E|}}(\sqrt{n}B)}{\int \rho(\sqrt{n}\tilde{\theta}; \sqrt{n}\theta_{n,E}^*, \Sigma_E) \rho(\Pi(\sqrt{n}\tilde{B}, U); 0_d, \Omega) \mathbb{1}_{\mathbb{R}_+^{|E|}}(\sqrt{n}\tilde{B}) d\tilde{\theta} d\tilde{B}}. \end{aligned} \tag{17}$$

Take the numerator, ignoring the Jacobian and indicator functions for now, following the

proof of Proposition 2.4 in Huang et al. [2023a]:

$$\begin{aligned}
& \rho(\sqrt{n}\bar{\theta}_{n,E}; \sqrt{n}\theta_{n,E}^*, \Sigma_E) \rho(\Pi(\sqrt{n}B, U); 0_d, \Omega) \\
&= c_E \exp \left\{ -\frac{1}{2} (\sqrt{n}\bar{\theta}_{n,E} - \sqrt{n}\theta_{n,E}^*)^\top \Sigma_E^{-1} (\sqrt{n}\bar{\theta}_{n,E} - \sqrt{n}\theta_{n,E}^*) \right\} \\
& \quad \times \exp \left\{ -\frac{1}{2} (C_1 \sqrt{n}\bar{\theta}_{n,E} + C_2 \sqrt{n}B + f(U; \sqrt{n}\bar{\theta}_\perp))^\top \Omega^{-1} (C_1 \sqrt{n}\bar{\theta}_{n,E} + C_2 \sqrt{n}B + f(U; \sqrt{n}\bar{\theta}_\perp)) \right\} \\
&= c_E \exp \left\{ -\frac{1}{2} \left[n\bar{\theta}_{n,E}^\top \Sigma_E^{-1} \bar{\theta}_{n,E} - 2n\bar{\theta}_{n,E}^\top \Sigma_E^{-1} \theta_{n,E}^* + n\theta_{n,E}^{*\top} \Sigma_E^{-1} \theta_{n,E}^* \right. \right. \\
& \quad + 2C_2 \sqrt{n}B^\top \Omega^{-1} (C_1 \sqrt{n}\bar{\theta}_{n,E} + f(U; \sqrt{n}\bar{\theta}_\perp)) + (C_1 \sqrt{n}\bar{\theta}_{n,E} + f(U; \sqrt{n}\bar{\theta}_\perp))^\top \Omega^{-1} (C_1 \sqrt{n}\bar{\theta}_{n,E} \\
& \quad \left. \left. + f(U; \sqrt{n}\bar{\theta}_\perp)) + nB^\top C_2^\top \Omega^{-1} C_2 B \right] \right\} \\
&= c_E \exp \left\{ -\frac{1}{2} n\bar{\theta}_{n,E}^\top \Sigma_E^{-1} \bar{\theta}_{n,E} + n\bar{\theta}_{n,E}^\top \Sigma_E^{-1} \theta_{n,E}^* - \frac{1}{2} n\theta_{n,E}^{*\top} \Sigma_E^{-1} \theta_{n,E}^* \right. \\
& \quad - \frac{1}{2} (\sqrt{n}B - P\sqrt{n}\bar{\theta}_{n,E} - q)^\top \Delta^{-1} (\sqrt{n}B - P\sqrt{n}\bar{\theta}_{n,E} - q) \\
& \quad + \frac{1}{2} (n\bar{\theta}_{n,E}^\top P^\top \Delta^{-1} P \bar{\theta}_{n,E} + 2\sqrt{n}\bar{\theta}_{n,E}^\top \Delta^{-1} \Delta P^\top \Delta^{-1} q + q \Delta^{-1} q) \\
& \quad \left. - \frac{1}{2} (n\bar{\theta}_{n,E}^\top C_1^\top \Omega^{-1} C_1 \bar{\theta}_{n,E} + 2\sqrt{n}\bar{\theta}_{n,E}^\top \Delta^{-1} \Delta C_1^\top \Omega^{-1} f(U; \sqrt{n}\bar{\theta}_\perp) + f(U; \sqrt{n}\bar{\theta}_\perp)^\top \Omega^{-1} f(U; \sqrt{n}\bar{\theta}_\perp)) \right\} \\
&= c_E \exp \left\{ -\frac{1}{2} n\bar{\theta}_{n,E}^\top Z^{-1} \bar{\theta}_{n,E} + \sqrt{n}\bar{\theta}_{n,E}^\top Z^{-1} m + n\bar{\theta}_{n,E}^\top Z^{-1} L \theta_{n,E}^* \right. \\
& \quad \left. + c(\sqrt{n}\theta_{n,E}^*) - \frac{1}{2} (\sqrt{n}B - P\sqrt{n}\bar{\theta}_{n,E} - q)^\top \Delta^{-1} (\sqrt{n}B - P\sqrt{n}\bar{\theta}_{n,E} - q) \right\} \\
&= c_E \exp \left\{ -\frac{1}{2} [(\sqrt{n}\bar{\theta}_{n,E} - L\sqrt{n}\theta_{n,E}^* + m)^\top Z^{-1} (\sqrt{n}\bar{\theta}_{n,E} - L\sqrt{n}\theta_{n,E}^* + m) \right. \\
& \quad - (L\sqrt{n}\theta_{n,E}^* + m)^\top Z^{-1} (L\sqrt{n}\theta_{n,E}^* + m)] + c(\theta_{n,E}^*) \\
& \quad \left. - \frac{1}{2} (\sqrt{n}B - P\sqrt{n}\bar{\theta}_{n,E} - q)^\top \Delta^{-1} (\sqrt{n}B - P\sqrt{n}\bar{\theta}_{n,E} - q) \right\} \\
&= d(\theta_{n,E}^*) \rho(\sqrt{n}\bar{\theta}_{n,E}; L\sqrt{n}\theta_{n,E}^* + m, Z) \rho(\sqrt{n}B; P\sqrt{n}\bar{\theta}_{n,E} + q, \Delta),
\end{aligned}$$

where

$$\begin{aligned}
c_E &= 1/[(2\pi)^{|E|+d} |\Sigma_E| |\Omega|]^{1/2} \\
c(\theta_{n,E}^*) &= q^\top \Delta^{-1} q - \frac{1}{2} f(U; \sqrt{n}\bar{\theta}_\perp)^\top \Omega^{-1} f(U; \sqrt{n}\bar{\theta}_\perp) - \frac{1}{2} n\theta_{n,E}^{*\top} \Sigma_E^{-1} \theta_{n,E}^*; \\
d(\theta_{n,E}^*) &= c_E \exp \{ -(L\sqrt{n}\theta_{n,E}^* + m)^\top Z^{-1} (L\sqrt{n}\theta_{n,E}^* + m) + c(\theta_{n,E}^*) \}.
\end{aligned}$$

Substitute this new form into (17) and the proof is complete. \square

Proof of Theorem 2. Define the reparameterization $\eta_{n,E} = Z^{-1}(L\sqrt{n}\theta_{n,E}^* + m)$ and the function $h : \mathbb{R}^{|E|} \times \mathbb{R}^{|E|} \rightarrow \mathbb{R}$ such that

$$h(\tilde{\theta}, \tilde{b}) = \frac{1}{2}\tilde{\theta}^\top Z^{-1}\tilde{\theta} + \frac{1}{2}(\tilde{b} - P\tilde{\theta} - q)^\top \Delta^{-1}(\tilde{b} - P\tilde{\theta} - q) + \phi_{\mathcal{K}}(\tilde{b}).$$

The convex conjugate of $h(\cdot)$ at $(\eta_{n,E}^\top, 0_{|E|}^\top)^\top$ is

$$h^*(\eta_{n,E}, 0_{|E|}) = \sup_{\tilde{\theta}, \tilde{b}} \{\tilde{\theta}^\top \eta_{n,E} - h(\tilde{\theta}, \tilde{b})\}.$$

Now we can rewrite the log-likelihood in (9) as

$$-\frac{1}{2}n\bar{\theta}_{n,E}^\top Z^{-1}\bar{\theta}_{n,E} + \sqrt{n}\bar{\theta}_{n,E}^\top \eta_{n,E} - h^*(\eta_{n,E}, 0_{|E|}). \quad (18)$$

The maximizer of this likelihood with respect to the parameter $\eta_{n,E}$ is

$$\eta_{n,E}^* = \operatorname{argmin}_{\eta_{n,E}} \{h^*(\eta_{n,E}, 0_{|E|}) - \sqrt{n}\bar{\theta}_{n,E}^\top \eta_{n,E}\}. \quad (19)$$

Reverting to the original parameterization

$$\sqrt{n}\tilde{\theta}_{n,E} = L^{-1}Z\eta_{n,E}^* - L^{-1}m. \quad (20)$$

Now solve the optimization in (19):

$$\min_{\eta_{n,E}, \eta'_{n,E}, u} \{h^*(\eta'_{n,E}, u) - \sqrt{n}\bar{\theta}_{n,E}^\top \eta_{n,E}\} \quad \text{such that } \eta_{n,E} = \eta'_{n,E}; \quad u = 0_{|E|}$$

using the Lagrange multipliers θ, b :

$$\begin{aligned} \mathcal{L}(\theta, b; \eta_{n,E}, \eta'_{n,E}, u) &= \theta^\top (\eta_{n,E} - \eta'_{n,E}) - b^\top u + h^*(\eta'_{n,E}, u) - \sqrt{n}\bar{\theta}_{n,E}^\top \eta_{n,E} = \\ &= [-\theta^\top \eta'_{n,E} - b^\top u + h^*(\eta'_{n,E}, u)] + [\theta^\top \eta_{n,E} - \sqrt{n}\bar{\theta}_{n,E}^\top \eta_{n,E}]. \end{aligned}$$

Note that the minimizer of the first term over $(\eta'_{n,E}, u)$ is $-h(\theta, b)$ by the definition of conjugate function. Therefore

$$\begin{aligned} \max_{\theta, b} \min_{\eta_{n,E}, \eta'_{n,E}, u} [\mathcal{L}(\theta, b; \eta_{n,E}, \eta'_{n,E}, u)] &= \max_{\theta, b} [-h(\theta, b) - 1_{\sqrt{n}\bar{\theta}_{n,E}}(\theta)] \\ &= \min_{\theta, b} [h(\theta, b)] \quad \text{such that } \theta = \sqrt{n}\bar{\theta}_{n,E} \quad (21) \\ &= \min_{\theta, b} [h(\sqrt{n}\bar{\theta}_{n,E}, b)] \quad \text{where } b \in \mathbb{R}^{|E|}. \end{aligned}$$

The solution is

$$(\theta^*, b^*, \eta_{n,E}^*, \eta'_{n,E}, u^*) = \arg \max_{\theta, b} \min_{\eta_{n,E}, \eta'_{n,E}, u} \mathcal{L}(\theta, b; \theta_{n,E}, \eta'_{n,E}, u).$$

The Karush-Kuhn-Tucker conditions are

$$\nabla \mathcal{L} = 0 \implies \nabla h^*(\eta'_{n,E}, u^*) = \begin{pmatrix} \theta^* \\ b^* \end{pmatrix}.$$

By (21),

$$\begin{aligned} \theta^* &= \sqrt{n} \bar{\theta}_{n,E} \\ b^* &= b_n^*(\sqrt{n} \bar{\theta}_{n,E}) = \operatorname{argmin}_b \{h(\sqrt{n} \bar{\theta}_{n,E}, b)\}. \end{aligned}$$

Therefore, by inverting the Karush-Kuhn-Tucker conditions and using the above equalities,

$$(\eta'_{n,E}, u^*) = (\nabla h^*)^{-1}(\theta^*, b^*) = \nabla h(\theta^*, b^*) = \nabla h(\sqrt{n} \bar{\theta}_{n,E}, b^*).$$

The first $|E|$ rows are

$$\eta'_{n,E} = \frac{\partial h(\sqrt{n} \bar{\theta}_{n,E}, b^*)}{\partial (\sqrt{n} \bar{\theta}_{n,E})} = Z^{-1} \sqrt{n} \bar{\theta}_{n,E} + P^\top \Delta^{-1} (P \sqrt{n} \bar{\theta}_{n,E} + q - b^*).$$

Now substitute this into the maximum likelihood estimator definition in (20) and obtain the selective maximum likelihood estimator:

$$\begin{aligned} \sqrt{n} \tilde{\theta}_{n,E} &= L^{-1} Z \eta_{n,E}^* - L^{-1} m = \\ &= L^{-1} Z [Z^{-1} \sqrt{n} \bar{\theta}_{n,E} + P^\top \Delta^{-1} (P \sqrt{n} \bar{\theta}_{n,E} + q - b^*)] - L^{-1} m = \\ &= L^{-1} \sqrt{n} \bar{\theta}_{n,E} - L^{-1} m + \Sigma_E P^\top \Delta^{-1} [P \sqrt{n} \bar{\theta}_{n,E} + q - b_n^*(\sqrt{n} \bar{\theta}_{n,E})]. \end{aligned}$$

For the computation of the Fisher information matrix, define the derivatives

$$\begin{pmatrix} \tilde{\theta}^* \\ \tilde{b}^* \end{pmatrix} = \nabla h^*(\eta_{n,E}, 0_{|E|}) = (\nabla h)^{-1}(\eta_{n,E}, 0_{|E|}), \quad (22)$$

then obtain some useful derivatives:

$$\begin{aligned}
\frac{\partial \eta_{n,E}}{\partial \theta_{n,E}^*} &= \sqrt{n} Z^{-1} L = \sqrt{n} \Sigma_E^{-1}; \\
\frac{\partial}{\partial \eta_{n,E}} [-f(\eta_{n,E})] &= -\sqrt{n} \bar{\theta}_{n,E} + \frac{\partial}{\partial \eta_{n,E}} h^*(\eta_{n,E}, 0_{|E|}) = -\sqrt{n} \bar{\theta}_{n,E} + \tilde{\theta}^*; \\
-\nabla^2 f(\eta_{n,E}) &= \frac{\partial \tilde{\theta}^*}{\partial \eta_{n,E}}.
\end{aligned} \tag{23}$$

By (22),

$$\begin{pmatrix} \eta_{n,E} \\ 0_{|E|} \end{pmatrix} = \nabla h(\tilde{\theta}^*, \tilde{b}^*) = \begin{pmatrix} Z^{-1} \tilde{\theta}^* - P^\top \Delta^{-1} (\tilde{b}^* - P \tilde{\theta}^* - q) \\ \Delta^{-1} (\tilde{b}^* - P \tilde{\theta}^* - q) + \nabla \phi_{\mathcal{K}}(\tilde{b}^*) \end{pmatrix}. \tag{24}$$

Take the derivative with respect to $\eta_{n,E}$ of the first $|E|$ rows of (24),

$$\begin{aligned}
\frac{\partial \eta_{n,E}}{\partial \eta_{n,E}} &= \frac{\partial}{\partial \eta_{n,E}} (Z^{-1} \tilde{\theta}^* - P^\top \Delta^{-1} (\tilde{b}^* - P \tilde{\theta}^* - q)) \\
I_{|E|} &= (Z^{-1} + P^\top \Delta^{-1} P) \frac{\partial \tilde{\theta}^*}{\partial \eta_{n,E}} - P^\top \Delta^{-1} \frac{\partial \tilde{b}^*}{\partial \tilde{\theta}^*} \frac{\partial \tilde{\theta}^*}{\partial \eta_{n,E}} \\
\frac{\partial \tilde{\theta}^*}{\partial \eta_{n,E}} &= (Z^{-1} + P^\top \Delta^{-1} P - P^\top \Delta^{-1} \frac{\partial \tilde{b}^*}{\partial \tilde{\theta}^*})^{-1}.
\end{aligned} \tag{25}$$

Now differentiate the last $|E|$ rows of (24) with respect to $\tilde{\theta}^*$:

$$\begin{aligned}
0_{|E|} &= \Delta^{-1} \frac{\partial \tilde{b}^*}{\partial \tilde{\theta}^*} - \Delta^{-1} P - \nabla^2 \phi_{\mathcal{K}}(\tilde{b}^*) \frac{\partial \tilde{b}^*}{\partial \tilde{\theta}^*} \\
\frac{\partial \tilde{b}^*}{\partial \tilde{\theta}^*} &= (\Delta^{-1} + \nabla^2 \phi_{\mathcal{K}}(\tilde{b}^*))^{-1} \Delta^{-1} P.
\end{aligned}$$

Substitute the above into (25):

$$\frac{\partial \tilde{\theta}^*}{\partial \eta_{n,E}} = (Z^{-1} + P^\top \Delta^{-1} P - P^\top \Delta^{-1} [\Delta^{-1} + \nabla^2 \phi_{\mathcal{K}}(\tilde{b}^*)]^{-1} \Delta^{-1} P)^{-1}. \tag{26}$$

Note that the reparameterized log-likelihood in (18) is proportional to

$$f(\eta_{n,E}) = \sqrt{n} \bar{\theta}_{n,E}^\top \eta_{n,E} - h^*(\eta_{n,E}, 0_{|E|}).$$

Now we take the Hessian:

$$\frac{\partial^2}{\partial \theta_{n,E}^* \partial \theta_{n,E}^{*\top}} [-f(\eta_{n,E})] = \frac{\partial \eta_{n,E}}{\partial \theta_{n,E}^*} \left[\frac{\partial^2 (-f(\eta_{n,E}))}{\partial \eta_{n,E} \partial \eta_{n,E}^\top} \right] \frac{\partial \eta_{n,E}}{\partial \theta_{n,E}^*}.$$

By the derivatives in (23),

$$\frac{\partial^2}{\partial \theta_{n,E}^* \partial \theta_{n,E}^{*\top}} [-f(\eta_{n,E})] = n \Sigma_E^{-1} \left[\frac{\partial \tilde{\theta}^*}{\partial \eta_{n,E}} \right] \Sigma_E^{-1}.$$

Now plug $\sqrt{n}\bar{\theta}_{n,E}$ into the unknown $\tilde{\theta}^*$ and therefore $\tilde{b}^* = b_n(\sqrt{n}\bar{\theta}_{n,E})$ into (26) and define

$$M^{-1} = (Z^{-1} + P^\top \Delta^{-1} P - P^\top \Delta^{-1} [\Delta^{-1} + \nabla^2 \phi_{\mathcal{K}}(b_n(\sqrt{n}\bar{\theta}_{n,E}))]^{-1} \Delta^{-1} P)^{-1}.$$

Finally, the Fisher information matrix is $n \Sigma_E^{-1} M^{-1} \Sigma_E^{-1}$. \square

Proof of Proposition 4. Note that the first derivative of the elastic net penalty is $\mathcal{P}'_\gamma(x) = \lambda_n[\gamma + (1 - \gamma)x]$, therefore the subgradient of the penalty needs to be computed appropriately with the corresponding Karush-Kuhn-Tucker conditions. The Karush-Kuhn-Tucker conditions are

$$\begin{aligned} D_p^\top \text{vec}(S_n - W_n - \hat{\Theta}_{n,\lambda_n}^{-1} + \gamma \mathcal{P}' + \lambda_n(1 - \gamma) \hat{\Theta}_{n,\lambda_n}) &= 0 \\ \frac{\sqrt{n}}{2} D_p^\top \text{vec}(S_n - \hat{\Theta}_{n,\lambda_n}^{-1}) - \sqrt{n} \omega_n + \frac{\sqrt{n}}{2} \gamma D_p^\top \text{vec}(\hat{\mathcal{P}}') + \frac{\sqrt{n}}{2} \lambda_n(1 - \gamma) D_p^\top \text{vec}(\hat{\Theta}_{n,\lambda_n}) &= 0 \\ n^{-1/2} \frac{\partial \ell_n(\hat{\Theta}_{n,\lambda_n}; X)}{\partial \text{vh}(\Theta)} - \sqrt{n} \omega_n + \frac{\sqrt{n}}{2} \gamma D_p^\top \text{vec}(\hat{\mathcal{P}}') + \frac{\sqrt{n}}{2} \lambda_n(1 - \gamma) D_p^\top \text{vec}(\hat{\Theta}_{n,\lambda_n}) &= 0. \end{aligned}$$

Therefore

$$\begin{aligned} \sqrt{n} \omega_n &= n^{-1/2} \frac{\partial \ell_n(\hat{\Theta}_{n,\lambda_n}; X)}{\partial \text{vh}(\Theta)} + \frac{\sqrt{n}}{2} \gamma D_p^\top \text{vec}(\hat{\mathcal{P}}') + \frac{\sqrt{n}}{2} \lambda_n(1 - \gamma) D_p^\top \text{vec}(\hat{\Theta}_{n,\lambda_n}) \\ &= (-J_{n,E} J_{n,EE}^{-1} H_{n,EE}) \sqrt{n} \bar{\theta}_{n,E} + H_{n,E} \sqrt{n} \text{diag}(S) B + \sqrt{n} \bar{\theta}_\perp \\ &\quad + \frac{\sqrt{n}}{2} \gamma D_p^\top \text{vec}(\hat{\mathcal{P}}') + \frac{\sqrt{n}}{2} \lambda_n(1 - \gamma) D_p^\top \text{vec}(\hat{\Theta}_{n,\lambda_n}) \\ &= (-J_{n,E} J_{n,EE}^{-1} H_{n,EE}) \sqrt{n} \bar{\theta}_{n,E} + H_{n,E} \sqrt{n} \text{diag}(S) B + \sqrt{n} \bar{\theta}_\perp \\ &\quad + \frac{\sqrt{n}}{2} \gamma D_p^\top \text{vec}(\hat{\mathcal{P}}') + \frac{\sqrt{n}}{2} \lambda_n(1 - \gamma) D_p^\top D_p \text{vh}(\hat{\Theta}_{n,\lambda_n}) \\ &= (-J_{n,E} J_{n,EE}^{-1} H_{n,EE}) \sqrt{n} \bar{\theta}_{n,E} + H_{n,E} \sqrt{n} \text{diag}(S) B + \sqrt{n} \bar{\theta}_\perp \\ &\quad + \frac{\sqrt{n}}{2} \gamma D_p^\top \text{vec}(\hat{\mathcal{P}}') + \frac{\sqrt{n}}{2} \lambda_n(1 - \gamma) D_p^\top D_p \text{diag}(S) B \\ &= (-J_{n,E} J_{n,EE}^{-1} H_{n,EE}) \sqrt{n} \bar{\theta}_{n,E} + \sqrt{n} (H_{n,E} + K_{n,E}) \text{diag}(S) B + \frac{\sqrt{n}}{2} \gamma D_p^\top \text{vec}(\hat{\mathcal{P}}') + \sqrt{n} \bar{\theta}_\perp \end{aligned}$$

\square

References

- Donald WK Andrews. Inconsistency of the bootstrap when a parameter is on the boundary of the parameter space. *Econometrica*, pages 399–405, 2000.
- Soham Bakshi, Yiling Huang, Snigdha Panigrahi, and Walter Dempsey. Inference with randomized regression trees. *Unpublished*, 2024. arXiv:2412.20535.
- A. Barrat, M. Barthélemy, R. Pastor-Satorras, and A. Vespignani. The architecture of complex weighted networks. *Proceedings of the National Academy of Sciences*, 101(11):3747–3752, 2004. doi: 10.1073/pnas.0400087101. URL <https://www.pnas.org/doi/abs/10.1073/pnas.0400087101>.
- Daniel Castro, Filipa Ferreira, Inês de Castro, Ana Rita Rodrigues, Marta Correia, Josefina Ribeiro, and Tiago Bento Ferreira. The differential role of central and bridge symptoms in deactivating psychopathological networks. *Frontiers in psychology*, 10:2448, 2019.
- Giuseppe Cavaliere, Heino Bohn Nielsen, and Anders Rahbek. On the consistency of bootstrap testing for a parameter on the boundary of the parameter space. *Journal of Time Series Analysis*, 38(4):513–534, 2017.
- Zhang J Chen, Yong He, Pedro Rosa-Neto, Jurgen Germann, and Alan C Evans. Revealing modular architecture of human brain structural networks by using cortical thickness from MRI. *Cerebral cortex*, 18(10):2374–2381, 2008.
- Gabriel del Rio, Dirk Koschützki, and Gerardo Coello. How to identify essential genes from molecular networks? *BMC systems biology*, 3:1–12, 2009.
- Rahul S Desikan, Florent Ségonne, Bruce Fischl, Brian T Quinn, Bradford C Dickerson, Deborah Blacker, Randy L Buckner, Anders M Dale, R Paul Maguire, Bradley T Hyman, et al. An automated labeling system for subdividing the human cerebral cortex on MRI scans into gyral based regions of interest. *Neuroimage*, 31(3):968–980, 2006.

- Vo Nguyen Le Duy and Ichiro Takeuchi. Parametric programming approach for more powerful and general Lasso selective inference. In *Proceedings of The 24th International Conference on Artificial Intelligence and Statistics*, pages 901–909. PMLR, 2021.
- William Fithian, Dennis Sun, and Jonathan Taylor. Optimal inference after model selection. *Unpublished*, 2017. URL <https://arxiv.org/abs/1410.2597>. arXiv:1410.2597.
- Linton C. Freeman. Centrality in social networks conceptual clarification. *Social Networks*, 1(3):215–239, 1978. ISSN 0378-8733. doi: [https://doi.org/10.1016/0378-8733\(78\)90021-7](https://doi.org/10.1016/0378-8733(78)90021-7). URL <https://www.sciencedirect.com/science/article/pii/0378873378900217>.
- Tobias Freidling, Qingyuan Zhao, and Zijun Gao. Selective randomization inference for adaptive experiments. *Unpublished*, 2024. arXiv:2405.07026.
- Jerome Friedman, Trevor Hastie, and Robert Tibshirani. Sparse inverse covariance estimation with the graphical lasso. *Biostatistics*, 9(3):432–441, 2008.
- Michael D Greicius, Kaustubh Supekar, Vinod Menon, and Robert F Dougherty. Resting-state functional connectivity reflects structural connectivity in the default mode network. *Cerebral cortex*, 19(1):72–78, 2009.
- Sofia Guglielmini and Gerda Claeskens. Asymptotic post-selection inference for regularized graphical models. *Statistics and Computing*, 35:36, 2025.
- David A Harville. *Matrix Algebra from a Statistician’s Perspective*. Taylor & Francis, 1998.
- Yiling Huang, Snigdha Panigrahi, and Walter Dempsey. Selective inference for sparse graphs via neighborhood selection. *Unpublished*, 2023a. arXiv:2312.16734.
- Yiling Huang, Sarah Pirenne, Snigdha Panigrahi, and Gerda Claeskens. Selective inference using randomized group lasso estimators for general models. *Unpublished*, 2023b. arXiv:2306.13829.

- Peter J Huber. *Robust Statistics*. Wiley Series in Probability and Mathematical Statistics. Wiley, New York, 1981.
- Jana Janková and Sara van de Geer. Confidence intervals for high-dimensional inverse covariance estimation. *Electronic Journal of Statistics*, 9(1):1205–1229, 2015.
- Steven G. Johnson. The NLOpt nonlinear-optimization package. <https://github.com/stevengj/nlopt>, 2007.
- Payton J Jones, Ruofan Ma, and Richard J McNally. Bridge centrality: a network approach to understanding comorbidity. *Multivariate behavioral research*, 56(2):353–367, 2021.
- Danijel Kivaranovic and Hannes Leeb. On the length of post-model-selection confidence intervals conditional on polyhedral constraints. *Journal of the American Statistical Association*, 116(534):845–857, 2021. doi: 10.1080/01621459.2020.1732989.
- Solt Kovács, Tobias Ruckstuhl, Helena Obrist, and Peter Bühlmann. Graphical elastic net and target matrices: Fast algorithms and software for sparse precision matrix estimation. *Unpublished*, 2021. arXiv:2101.02148.
- Jason D. Lee, Dennis L. Sun, Yuekai Sun, and Jonathan E. Taylor. Exact post-selection inference, with application to the lasso. *The Annals of Statistics*, 44(3):907–927, 2016.
- Fred C Leone, Lloyd S Nelson, and RB Nottingham. The folded normal distribution. *Technometrics*, 3(4):543–550, 1961.
- Jan R. Magnus and H. Neudecker. Matrix differential calculus with applications to simple, Hadamard, and Kronecker products. *Journal of Mathematical Psychology*, 29(4):474–492, 1985.
- Daniel S Marcus, Tracy H Wang, Jamie Parker, John G Csernansky, John C Morris, and Randy L Buckner. Open Access Series of Imaging Studies (OASIS): cross-sectional

- MRI data in young, middle aged, nondemented, and demented older adults. *Journal of cognitive neuroscience*, 19(9):1498–1507, 2007.
- Daniel S Margulies, Justin L Vincent, Clare Kelly, Gabriele Lohmann, Lucina Q Uddin, Bharat B Biswal, Arno Villringer, F Xavier Castellanos, Michael P Milham, and Michael Petrides. Precuneus shares intrinsic functional architecture in humans and monkeys. *Proceedings of the National Academy of Sciences*, 106(47):20069–20074, 2009.
- Michael A Martin. Bootstrap hypothesis testing for some common statistical problems: A critical evaluation of size and power properties. *Computational Statistics & Data Analysis*, 51(12):6321–6342, 2007.
- Anna C Neufeld, Lucy L Gao, and Daniela M Witten. Tree-values: selective inference for regression trees. *Journal of Machine Learning Research*, 23(305):1–43, 2022.
- Snigdha Panigrahi and Jonathan Taylor. Scalable methods for Bayesian selective inference. *Electronic Journal of Statistics*, 12:2355–2400, 2018.
- Snigdha Panigrahi and Jonathan Taylor. Approximate selective inference via maximum likelihood. *Journal of the American Statistical Association*, 118(544):2810–2820, 2023.
- Snigdha Panigrahi, Peter W MacDonald, and Daniel Kessler. Approximate post-selective inference for regression with the group lasso. *Journal of machine learning research*, 24(79):1–49, 2023.
- Snigdha Panigrahi, Kevin Fry, and Jonathan Taylor. Exact selective inference with randomization. *Biometrika*, 111(4):1109–1127, 2024.
- Richard R Picard and Kenneth N Berk. Data splitting. *The American Statistician*, 44(2):140–147, 1990.
- M. J. D. Powell. A direct search optimization method that models the objective and constraint functions by linear interpolation. In *Advances in Optimization and Numerical*

- Analysis*, volume 275 of *Mathematics and Its Applications*, pages 51–67. Springer, 1994.
doi: 10.1007/978-94-015-8330-5_4.
- Donald J Robinaugh, Alexander J Millner, and Richard J McNally. Identifying highly influential nodes in the complicated grief network. *Journal of abnormal psychology*, 125(6):747, 2016.
- Jorge Sepulcre, Hesheng Liu, Tanveer Talukdar, Iñigo Martincorena, B. T. Thomas Yeo, and Randy L. Buckner. The organization of local and distant functional connectivity in the human brain. *PLOS Computational Biology*, 6(6):1–15, 06 2010. doi: 10.1371/journal.pcbi.1000808. URL <https://doi.org/10.1371/journal.pcbi.1000808>.
- Olaf Sporns. The human connectome: a complex network. *Annals of the new York Academy of Sciences*, 1224(1):109–125, 2011.
- Shriram Srinivasan and Nishant Panda. What is the gradient of a scalar function of a symmetric matrix? *Indian Journal of Pure and Applied Mathematics*, 54(3):907–919, 2023.
- Tingni Sun and Cun-Hui Zhang. Sparse matrix inversion with scaled lasso. *The Journal of Machine Learning Research*, 14(1):3385–3418, 2013.
- Jonathan Taylor and Robert Tibshirani. Post-selection inference for ℓ_1 -penalized likelihood models. *The Canadian Journal of Statistics*, 46(1):41–61, 2018.
- Xiaoying Tian and Jonathan Taylor. Selective inference with a randomized response. *The Annals of Statistics*, 46(2):679–710, 2018.
- Charles F Van Loan and Nikos Pitsianis. *Approximation with Kronecker products*. Springer, 1993.